Applied Energy 235 (2019) 1427–1446

Contents lists available at ScienceDirect

Applied Energy

journal homepage: www.elsevier.com/locate/apenergy

A life cycle assessment-based multi-objective optimization of the purchased, solar, and wind energy for the grocery, perishables, and general merchandise multi-facility distribution center network

Jasmina Burek*, Darin W. Nutter

Department of Mechanical Engineering, University of Arkansas, 863 W. Dickson St., Fayetteville, AR 72701, USA

HIGHLIGHTS

- Pairwise comparison showed differences between distribution centers locations.
- The good, the better, and the zero energy distribution centers were defined.
- The multi-objective optimization showed feasible solar and wind energy solutions.
- One optimal solution did not fit all distribution center types and locations.
- The zero energy distribution centers showed a fivefold climate change reduction.

GRAPHICAL ABSTRACT

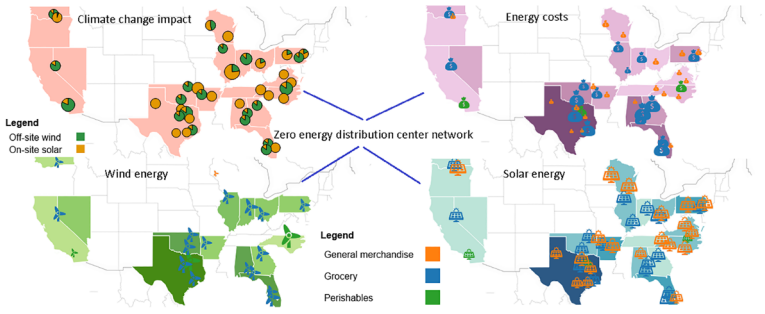

ARTICLE INFO

Keywords:
Refrigerated warehouse
Non-refrigerated warehouse
Food distribution center
Zero energy building
Life cycle assessment
Multi-objective optimization

ABSTRACT

Walmart Inc., the U.S. and world's largest grocery retailer, owns a perishables, grocery, and general merchandise distribution center network, which stores and distributes refrigerated and non-refrigerated food. Finding cost-effective strategies to implement solar and wind-powered electricity in their distribution centers was the central objective of this research. The study analyzed the tradeoffs and effects on costs and climate change impact related to the increase of renewable energy use in the distribution centers. The research combined the life cycle assessment and quantitative methods including the Monte Carlo uncertainty analysis and the multi-objective optimization. A life cycle assessment-based multi-objective optimization model was built to find cost-effective strategies to minimize fossil energy use and mitigate the impact of the Walmart Inc. distribution center network on climate change. The bi-objective and the triple-objective optimization included a number of combinations of minimal costs, non-renewable fossil energy use, and climate change impact criteria. The results of the multi-objective optimizations were Pareto-optimal solutions obtained by weighing the importance of chosen criteria from the baseline to the zero energy scenarios. A selection of the Pareto-optimal solutions included the good, the better, and the zero energy building scenarios. A better building was a Pareto-optimal set of buildings, which demonstrated superiority from the life cycle assessment perspective. The superiority of Pareto-optimal solutions was evaluated using the Monte Carlo pairwise comparison. The good distribution centers were characterized by the Pareto-optimal solutions between the baseline and the better distribution centers. Finally, the zero energy general merchandise distribution centers were mostly the Pareto-optimal solutions with a 100% share of solar energy. For the zero energy grocery and perishables distribution centers the solutions were a combination of

* Corresponding author.
E-mail address: jburek@uark.edu (J. Burek).

https://doi.org/10.1016/j.apenergy.2018.11.042
Received 27 July 2018; Received in revised form 10 October 2018; Accepted 10 November 2018
Available online 26 November 2018

solar and supplemental wind energy because refrigerated warehouses are more energy intensive. The study provided the benchmark results that may improve distribution centers and other buildings and a framework to test environmental and renewable energy policies in buildings.

1. Introduction

In the United States, 30% of commercial building energy is used inefficiently or unnecessarily, due to overcooling as one of the contributing factors [1]. Energy savings are the most important metrics of buildings' sustainability because the operational energy consumption is both the primary cost and the primary environmental impact driver [2]. Maximizing building energy efficiency and reducing system costs is necessary in an ongoing effort to improve the operation of buildings [3]. Specific to refrigerated warehouses, the use of cold thermal energy storage is known as a prominent technology to reduce electricity consumption [4]. The cold thermal energy storage system could reduce the electricity consumption by 4.4% and operational costs by 20.5% in refrigerated warehouses [4]. An alternative to improve refrigerated warehouse sustainability is by using renewable energy [5]. In their research, Fikiin et al. [6] concluded there were promising solutions to include renewable energy in refrigerated warehouses, in combination with the energy storage. The results of a case study showed that the photovoltaic installation can lead to both yearly total cost and energy savings [7]. However, these studies did not include the life cycle assessment (LCA), and thus, the reported reductions over the entire life cycle might be lower.

Recent studies have demonstrated that finding optimal cost-effective solutions for energy efficiency [8] and renewable energy consumption [9] in buildings were often solved using the single-objective and multi-objective optimization (MOO) methods [10]. In addition, mitigating stress on the environment by encouraging energy and resource-efficient buildings has become a part of green building certification programs such as Leadership in Energy and Environmental Design (LEED) [11]. Thus, to make informed choices and determine the best course of action towards green buildings, one might consider multiple criteria [12]. Often, the criteria are conflicting, for example, achieving the zero energy building may increase the building's costs [13], and vice versa, the increased costs and environmental impacts of building products such as insulation may decrease operational energy use [14]. Thus, potential tradeoffs between building's sustainability, efficiency, and costs need to be considered and evaluated [15].

The MOO is a method that can solve problems involving several competing objectives simultaneously and enable tradeoffs analysis. Various authors used the MOO to optimize different building systems including the addition of (1) solar panels [16], (2) the battery storage [17], (3) biomass gasification in the building's cooling, heating, and power systems (CHPSs) [18], and (4) solid oxide fuel cells for combined CHPSs [10]. In addition, several authors used the MOO to (1) retrofit existing building envelopes and achieve improved energy efficiency [8], (2) provide alternative building designs [12], (3) evaluate cogeneration and solar energy in a mix of buildings' energy suppliers [9], and (4) improve the energy efficiency of the buildings [10].

Many researchers have focused on minimizing buildings' energy consumption and costs. The three main objectives in one research study were to minimize (1) electricity consumption, (2) retrofitting costs of the building envelope, and (3) capital costs of photovoltaics [8]. Other authors maximized energy savings and cost-effectiveness and minimized a payback period of retrofitting [3]. Some authors focused only on minimizing the costs of photovoltaic and battery storage systems [17]. In some cases, authors included objective functions that minimized daylight factors and thermal requirements for building cost-effective energy optimization in the early design stage [19]. In addition to economic and energy efficiency objectives, some authors included environmental impacts; for example, one study minimized a building's total cost and annual carbon emissions of the combined CHPS [10]. Also, in one study, the MOO criteria was the aggregated total environmental impact potential of the building [12]. One study analyzed tradeoffs of minimizing different types of impacts including the non-renewable cumulative energy demand, greenhouse gas (GHG) emissions, acidification, and eutrophication [9]. Technologies used to improve the energy consumption and environmental impacts of building were, for example, (1) a wall and roof insulation and solar panels [8], (2) solid oxide fuel cells [10] (3) cogeneration [20], (4) biomass gasification [18], and (5) lighting, air-conditioning, and geyser interventions [3].

In recent years, the building optimization problems combined the LCA and the MOO. Noteworthy examples of such research included the LCA-based MOO of (1) building retrofitting [3,16], (2) a solar-assisted hybrid combined CHPS [21], and (3) the biomass CHPS [18]. The LCA method was used in single-optimization problems (1) to reduce the environmental impacts of a building's hybrid combined CHPS [21] and (2) to evaluate the effectiveness of greenhouse gas (GHG) emission reduction strategies in the building sector [22]. In multi-objective problems, the LCA method was applied to (1) increase renewable energy use in building CHPSs [18,21], and (2) improve building's energy efficiency through retrofitting [16].

The authors of previous research also used the MOO to improve sustainability of food distribution by finding feasible transportation routes, which minimized the post-processing transportation GHG emissions and the total costs of the food distribution supply chain [23]. However, the research did not include distribution centers (DCs) and retail centers (RCs) such as supermarkets, which play a significant role in the environmental performance of the food post-processing distribution [24].

Even though the published studies showed a broadening of the LCA research in the building and construction sector, as shown in compressive reviews written by Chau et al. [25], Abd Rashid et al. [26], and Cabeza et al. [27]; little LCA research has been done on DCs and supermarkets in the United States [28]. Richman, Pasqualini, and Kirsh [28] used the LCA to evaluate improvements in cold storage warehouses by defining the best roof insulation materials for each climate zone; however, this research did not include non-refrigerated food distribution centers [28].

One particular case of building studies called the zero energy buildings used the LCA method to evaluate renewable energy applications. To achieve the zero energy goal to use as much energy as can be generated onsite, buildings will often have to combine both energy efficiency and renewable energy generation [29]. The examples of the research that discussed the zero energy buildings included the techno-economic analysis of a hybrid zero emission building [30], the development of nearly zero energy buildings [31], and the discussion on steps to achieve the zero energy buildings [32]. Because of the low operational energy use in the residential sector, the zero energy buildings can be achieved using photovoltaic systems [31]. However, the concept of the zero energy warehouses is relatively new [33]. Refrigerated warehouses are energy intensive buildings and installing photovoltaics alone is often not sufficient to achieve the zero energy targets [7].

This research extends to the authors' studies on the environmental impacts of the Walmart Inc. DC network and environmental impacts of the food post-processing storage in warehouses and retailing [24,34]. DCs are warehouses used for (1) receiving bulk shipments from processors and manufacturers, (2) temporary storage, (3) grouping customized retail orders, and (4) distribution of goods to a point-of-sale. In

2012, the construction of RCs and warehouses accounted for 43% of the total commercial building revenue. In the same year, warehouses alone used 300,000 TJ of energy [35], which was about 7% of total energy use of all commercial buildings [36]. The top 75 North American food retailers have more than 49,890 RCs and 533 DCs with an estimated total area of 26,060,045 m^2 [37]. In 2017, refrigerated and non-refrigerated DCs were among the highest energy use facilities in the United States [38]. Refrigeration in commercial buildings accounted for the largest share of annual electricity consumption (14%), followed by ventilation (11.2%), lighting (10.6%), and space cooling (10.6%) [38].

The food supply chain consists of a network of suppliers such as farmers, manufacturers, distributors, retailers, and end customers [39]. Food distribution includes processes that occur between producers, retailers and customers, from packaging, transport, and storage to delivery to the consumer. Grocery, perishables, and general merchandise distribution centers, and retail centers are primary food distribution components [40], and have an important role in food distribution and sustainability. The role of DCs in the food supply chain is to move and store food and other products and to service retail centers such as supermarkets with food products [24]. Often, dry food could be stored for up to six months and refrigerated perishable food for more than a month before it was transported to the supermarket, which required high quantities of energy [24,41].

The Walmart Inc. is the largest retailer in the world [40]. In 2017, Walmart Inc. operated 173 DCs including 36 grocery DCs (GDCs), 6 perishables DCs (PDCs), and 42 general merchandise DCs (GMDCs) in the United States [37]. The Walmart Inc. GDCs were typically in the range from 78,968 to 92,903 m^2, and PDCs were in the range from 48,310 to 166,296 m^2. The GMDCs (102,193–111,855 m^2) included mechanized conveyors, which could be up to 39 km long [37]. The GDCs distribute refrigerated perishable food and dry food, the PDCs only refrigerated perishable food, and the GMDCs both non-food and dry food [37]. All DCs owned by a certain business are considered to be a distribution center network. In 2017, the combined floor area of the Walmart Inc. distribution and retail center network was estimated to be 72 million square meters, which was 1.36 times larger than the island of Manhattan [40].

A broad discussion about the Walmart Inc. DC network, the LCIA method used, input data, EnergyPlus [42] modeling, and comprehensive LCIA results were described in detail by Burek and Nutter [34]. In previous study, the authors assessed the environmental impacts of PDCs, GDCs, and GMDCs using the LCA method [34]. State-level resolution of the life cycle inventory (LCI) and the regional life cycle impact assessment (LCIA) method [34] were used, resulting in a comprehensive, multi-facility, and a whole-building LCA study about the Walmart Inc. distribution center network. The study focused on a full range of impact categories and analyzed the environmental impacts of buildings' individual operation systems such as lights, refrigeration, HVAC, conveyor systems, equipment and building material and construction [34]. Furthermore, the previous study tested the hypotheses that climate conditions, the year of the building's construction, building materials, state-level sources of electrical power, energy demand for refrigerated and non-refrigerated spaces, and conveyor lengths change the magnitude of environmental impacts of PDCs, GDCs, and GMDCs across the U.S. The research results identified similarities and differences in environmental impacts among the DCs. Also, the research investigated relationships between climate zones, energy demands, energy sources, building materials, and the environmental impacts of individual DCs [34]. The authors used the EnergyPlus [42] building simulation model based on warehouse survey data to obtain the energy consumption data such as lights, refrigeration, HVAC, and equipment for the Walmart Inc. PDCs, GDCs, and GMDCs [34]. The results have shown that the GDCs and PDCs have higher environmental impacts than the GMDCs due to refrigeration. The GDCs and PDCs used 950–982 MJ/m^2 per year and 1.3–17 m^3/m^2 of natural gas per year, whereas, GMDCs used 56–185 MJ/m^2 and 1.5–16 m^3/m^2 of natural gas per year. Both refrigeration and conveyors were energy intensive, but their energy consumption was less dependent on climate zones [34] than on differences in the state-level purchased electricity energy mix. These affected the climate change impact more than the climate zone, as shown in Fig. 1 [34]. The subsequent study about food storing and retailing had a different scope because it focused on the cold food supply chain relationships to refrigerated distribution center storages and on the supermarket departments' cold zones, and allocated storing and retailing impact to different food categories [24]. Previous studies did not include the Monte Carlo uncertainty analysis [24,34].

This study combined the LCA modeling with quantitative analysis including Monte Carlo uncertainty analysis and the MOO, as shown in

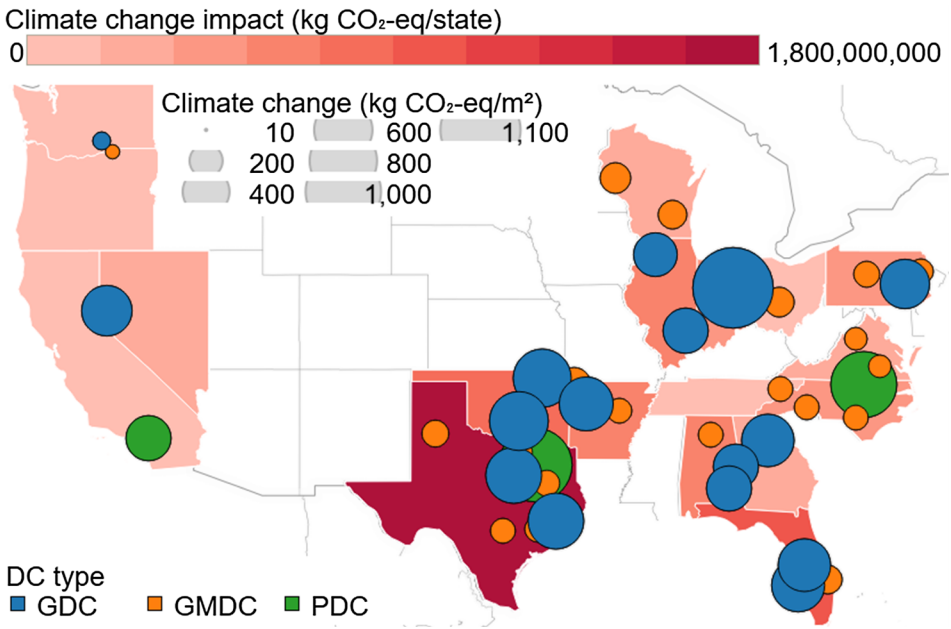

Fig. 1. The Walmart Inc. GDCs, GMDCs, and PDCs locations. The color of circles shows DC type. The size of circles shows the climate change impact of each building (kg CO_2-eq/m^2). The choropleth gradient map shows the total climate change impact of all Walmart Inc. DCs in a state (kg CO_2-eq/state).

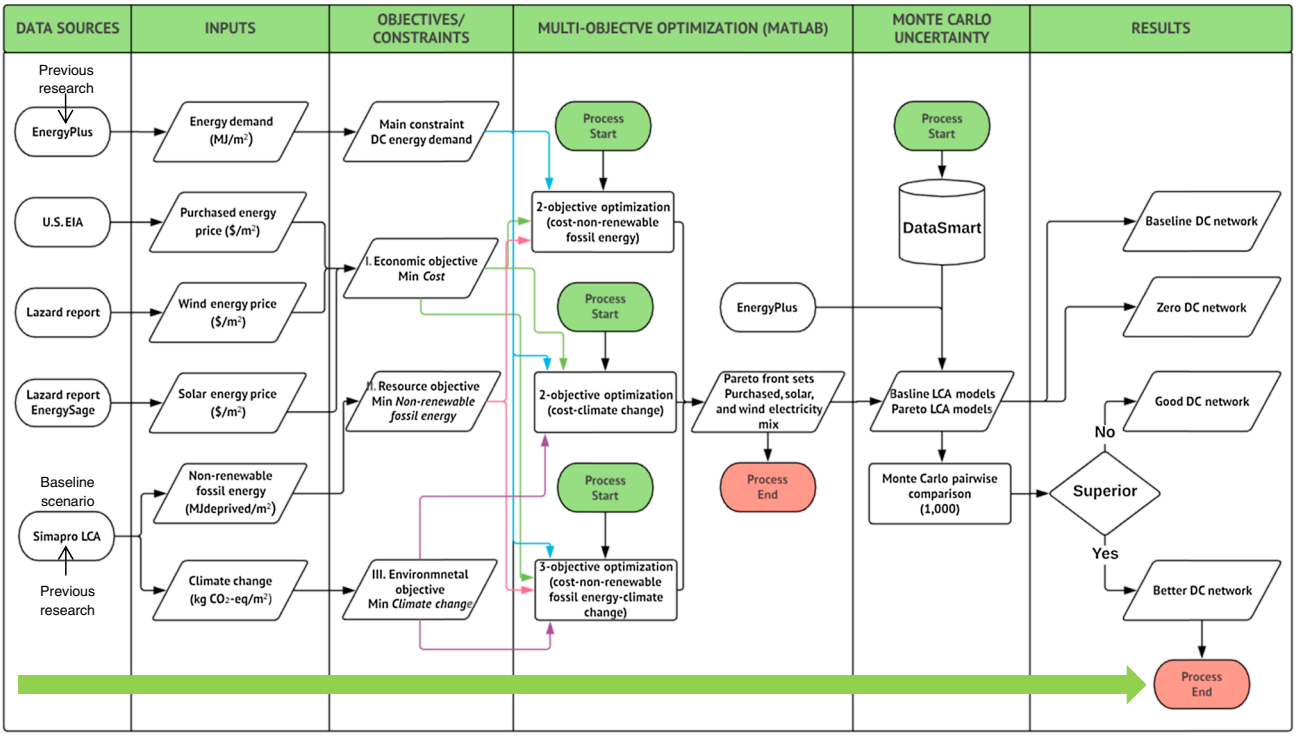

Fig. 2. The multi-objective optimization, the Monte Carlo uncertainty, and the Monte Carlo pairwise comparison flow diagram.

Fig. 2. The LCA models for the Walmart Inc. DC multi-facility network were taken from Burek and Nutter [34]. The locations of buildings, type of buildings, and climate change impact (kg CO_2-eq/m^2) for the baseline scenario are shown in Fig. 1. The whole-building LCIA results for the climate change impact and non-renewable fossil energy use presented in Burek and Nutter [34] were used as a baseline scenario.

Previous study focused on operations within the building and their environmental impacts [34]. This study focused on (1) assessing the overall environmental performance of the baseline DC network through the Monte Carlo uncertainty analysis and pairwise comparison, (2) finding cost-effective strategies to reduce their environmental impacts; and (3) finding the optimal zero energy and near zero climate change impact Walmart Inc. DC network. The electrical energy supply technologies chosen to reduce environmental impacts and to obtain the zero energy and near zero climate change impact DC network were new solar panels installed on the building rooftop and available electricity from new wind turbines at the nearby locations. We introduced wind turbines because the installed rooftop solar panels were not a sufficient energy source for the refrigerated warehouses to achieve zero energy targets due to their energy intensive operation [7]. The primary reasons to use solar and wind energy were a potential to rapidly reduce the buildings' dependency on fossil energy sources and mitigate the magnitude of their climate change impact.

The manuscript results should be of interest to readers in the areas of building sustainability, sustainability of food and distribution, LCA experts, MOO experts, policy makers, and to readers interested in the complex system analysis. Because the whole-building LCA is the new LEED credit [11], the results should be of interest to building code practitioners and experts. The research will also interest food distribution industry decision makers such as supply chain managers and may influence DCs retrofitting or future DC planning.

2. Goal and scope

The scope of the study included the LCA of the local, regional, and global DC network owned by the Walmart Inc., which is the same as in Burek and Nutter [34] for the baseline scenario. Several buildings were excluded because of missing cost data for optimization models. We started this study with the Monte Carlo uncertainty analysis and concluded that the largest uncertainties stemmed from the electricity generation. Then, we performed the Monte Carlo pairwise comparison to see if there were already buildings that perform better than the others in the network in terms of the life cycle fossil energy use.

The primary goals of this study were to (1) compare the environmental performance of the baseline DC in one state to a baseline DC of the same type in another state using the Monte Carlo pairwise comparison, which would enable finding and prioritizing improvements for locations that currently perform worse, (2) find tradeoffs between the building's energy consumption and an on-site energy production in a spatial LCA-based MOO model, which included economic (energy costs) and environmental outcomes (the non-renewable fossil energy use and the climate change impact) of the building's energy consumption and production, (3) find the LCA-based cost-effective strategies to reduce the impact of climate change and fossil energy resource use by installing flat roof solar panels at existing DCs, and/or by purchasing the offsite wind energy, (4) compare current building's energy use and optimum solutions using the LCA-based Monte Carlo pairwise comparisons, (5) find the least-costly DC network, which was superior to the existing DC network, and (6) find the optimal zero energy and near zero climate change impact DC network.

3. Materials and methods

The primary approaches used in this research were the LCA-based Monte Carlo pairwise comparison and the LCA-based MOO. The LCA is a standard method to assess the environmental impacts of products, processes, services, and whole buildings holistically, over the entire life cycle (i.e., from cradle-to-grave). Principles, requirements, and guidelines to perform LCA are given in the international standards: ISO 14040:2006, ISO 14044:2006, and ISO 14046:2014 [43–45]. Based on the previous research and discussion, the attributional LCA framework and process chain analysis were used. The attributional LCA is a system modeling approach in which the environmental impacts are divided among products based on the functional unit and according to

allocation principles (mass, energy, or economic). The process chain analysis includes itemized inputs and outputs for each LCA stage, as described in our previous work [34].

Fig. 2 shows a flow chart with data sources and methods used to perform this research. The columns 1, 2, 3, and 4 show data sources and steps necessary to perform the MOO. The primary sources of data about DC locations, LCIA results, and baseline DC LCA models for the Monte Carlo uncertainty analysis and MOO were taken from the previous study, as shown in Fig. 2, column 1 [34]. Data for purchased grid electricity costs, solar energy costs, and wind energy costs were obtained from literature, as shown in column 1. The column 2 shows the input data (i.e., cost, non-renewable fossil energy, and climate change) for the MOO, the column 3 shows objectives (i.e., cost, non-renewable fossil energy, and climate change) and constraints (i.e., source energy demand) used in MOO, and the column 4 shows a simplified bi- and triple-objective optimization model flow chart and selected solutions (i.e., Pareto-optimal bi- and triple-solutions' and associated purchased grid, wind, and solar energy mixes). The column 5 shows steps to perform the LCA-based Monte Carlo uncertainty analysis and the LCA-based Monte Carlo pairwise comparison. The column 6 shows the results of the MOO and the Monte Carlo pairwise comparison, which were used for tradeoff analyses.

An overview of the uncertainty in the input data of LCA models and Monte Carlo uncertainty analyses was performed first followed by a comparative study of the baseline DCs using the Monte Carlo pairwise comparisons. A Monte Carlo pairwise comparison between the baseline DCs was used to assess whether there are superior DCs in the existing GDC, PDC, and GMDC networks. Following the uncertainty analysis, a MOO of GDC, PDC, and GMDC networks was performed. The results of the MOO were further analyzed using the Monte Carlo pairwise comparison between the baseline DCs and the optimum results to find the good and the better DC networks, as shown in Fig. 2. In addition, the optimal zero energy and near zero climate change impact DC network was selected, as shown in Fig. 2.

3.1. Previous life cycle assessment research of the Walmart Inc. multi-facility PDC, GDC, and GMDC network

Our previous research presented a broad discussion about the environmental impacts of GDCs, PDCs, and GMDCs owned by Walmart Inc., and laid groundwork for this research [34]. For the purpose of this research, baseline process-LCA models of the GDCs, PDCs, and GMDCs were taken from previous work without modification and are available via Mendeley data [34]. Baseline process-LCA models were built using the Simapro© 8.4. software, which has the ability to perform LCIA, Monte Carlo uncertainty analysis, and Monte Carlo pairwise comparison [46]. The system boundary for the whole-building LCA included the building operation (i.e., refrigeration, refrigerant loss, lights, HVAC, machinery, and water consumption) and infrastructure (i.e., construction material production (envelope and insulation), building construction, and the end of the building life (building demolition and material disposal)). The functional unit of 1 m^2 of DC floor space was also adopted from the previous work [34]. Results of the LCA for the non-renewable fossil energy use and climate change impact (per functional unit of 1 m^2 floor area) were adopted from previous work and are reported in the Supporting Information (SI), Table S1 and in the SI, Excel document "1_Input data for multi-objective optimization.xlxs".

The number of DCs included in this study did not change significantly. The difficulty to find a reliable renewable energy cost data for Arizona, Missouri, Mississippi, Wyoming, Nebraska led to a decision to exclude those DC locations from the research.

The LCIA results for the baseline distribution center network adopted in this study were the climate change impact and the non-renewable fossil energy use. For most DCs, there was a correlation between the non-renewable energy use and the impact of climate change including Arkansas, Alabama, Arizona, Florida, Illinois, Nebraska, North Carolina, Oklahoma, Ohio, Oregon, Texas, Washington, and Wisconsin [34]. Replacing purchased grid electricity with renewable energy will simultaneously mitigate the non-renewable fossil energy use and the impacts of climate change. Thus, we expected the bi-objective results for a minimal cost and climate change optimization and a minimal cost and non-renewable fossil energy optimization to be similar.

3.2. The multi-objective optimization method

Various MOO methods were used previously for solving building's energy and the environmental impact reduction problems using the mixed-integer linear programming [22], the weighted sum method [8], the non-linear programming [47], stochastic and numerical MOO [10], and the differential evolution algorithm [48]. In most cases, the multi-objective problem was transformed into and solved as a single-objective optimization problem [21].

This study includes MOO using the goal programming known as the goal attainment method. The advantages of the goal attainment method are: (1) it is easier to implement than physical programming, (2) it is easier to code and is often used to solve practical cases, and (3) it is dependent on goal values chosen. The goal attainment problem involved reducing the value of a linear or non-linear function in order to attain the a priori specified vector which included goal values. A weight vector was used to indicate the relative importance of the goals. In addition, the goal attainment problem was subjected to linear and nonlinear constraints. In Matlab, the function used to solve the goal attainment problem is called fgoalattain [49]. We used the fgoalattain function to obtain our bi-optimization and triple-optimization results. The bi-optimization was performed at a minimal cost and minimal non-renewable fossil energy use criteria and at a minimal cost and minimal climate change impact. The triple-optimization was performed at a minimal cost, non-renewable fossil energy use, and climate change impact. The results of the bi- and triple-optimization were Pareto frontiers. The Pareto frontier yielded a set of Pareto-optimal results. Each Pareto-optimal result was a solution of the MOO which could not be improved without degrading the other objective value.

The multi-objective model finds a minimum of the problem specified by:

$$\underset{x,\gamma}{minimize}\gamma \quad such \quad that \quad \begin{cases} F(x) - weight\cdot\gamma \le goal \\ A\cdot x \le b \\ Aeq\cdot x = beq \\ lb \le x \le ub \end{cases}, \tag{1}$$

where F(x) was the objective function, the weight was the relevance of the objectives, the goal was a target value for each objective. A·x ≤ b and Aeq·x = beq were linear constraints, and lb and ub were lower and upper bounds, respectively.

3.2.1. Objective functions

The primary objective functions used in the bi-objective and triple-objective optimization models were cost, non-renewable fossil energy use, and climate change. These functions were chosen because the main goal of the study was to increase renewable energy in DCs. Replacing purchased grid electricity with renewable energy will simultaneously mitigate the non-renewable fossil energy and climate change impact, but potentially increase costs.

The minimum cost objective function shown in the Eq. (2) calculated how much of the electricity was purchased from the grid and how much was generated from on-site solar panels and nearby wind farms at the lowest cost.

$$\underset{x}{min} \quad C_{total} = C_{mix(in)}\cdot x_1 + C_{PV(out)}\cdot x_2 + C_{wind}\cdot x_3, \tag{2}$$

where $\underset{x}{min}\ C_{total}$ was the total purchased grid and renewable energy cost that needs to be minimized and x_1, x_2, and x_3 were variables representing shares of purchased grid, solar, and wind electricity, respectively. X_1, x_2, and x_3 variables were calculated using the MOO. $C_{mix(in)}$, $C_{PV(out)}$, and $C_{wind(in)}$ were cost coefficients, as shown in the SI, Table S1.

Costs of purchased grid ($C_{mix(in)}$), solar ($C_{PV(out)}$), and wind ($C_{wind(in)}$) energy were obtained from the U.S. Energy Information Administration (EIA) and the Lazard report [50,51], as shown in Fig. 2. In addition, state-level solar panel installation capital costs were obtained from the EnergySage report [52]. Costs coefficients ($C_{mix(in)}$) were based on the state electricity profiles for each location [50]. Washington state had the lowest retail price of electricity (0.077 $/kWh) and California had the highest (0.152 $/kWh). Electricity prices were multiplied by the DC's total electricity purchased grid (kWh/year) and divided by the building area (m^2). Non-refrigerated buildings had lower electricity consumption and lower electricity cost per whole building area. Refrigerated DCs' purchased grid electricity cost was between 81.5 $/$m^2$ (Washington) and 147 $/$m^2$ (California). Non-refrigerated DCs had electricity costs between 28 $/$m^2$ (Wisconsin) and 6 $/$m^2$ (Texas). $C_{mix(in)}$ calculation data and results are provided in the SI, Table S2.

Cost coefficients of solar energy ($C_{PV(out)}$) included the capital cost of installation of solar panels and the levelized solar electricity production cost. The Lazard report calculated the average U.S. comparative "levelized cost of energy" analysis for various technologies on a $/MWh basis, including subsidies, fuel costs, geography, and capital costs [51]. Only average levelized costs of solar electricity production were taken from the Lazard report [51]. Because capital costs of solar panel installation vary in different states and for different powers, we used data reported by the EnergySage [52]. The EnergySage reported minimum and maximum costs for 6 kW and 10 kW solar panels, after the Federal Investment Tax Credit was taken into account for 2018 in different states [52]. We assumed a 10 kW solar system and calculated the average cost for each state. For some locations, data was not available, thus, the average cost of reported states was used for Alabama, Arkansas, North Carolina, Nevada, Oklahoma, Tennessee, and Wisconsin. The capital costs ($/kW) were divided by a 25 year solar panel lifetime [51]. The average solar power per panel square meter of 0.161 (kW/m^2) was multiplied by the total roof area available for installation of solar panels. The result was the installation capacity (kW) for each DC [53]. Flat roofs are ideal for solar panels, but available space is less than the total building roof area. According to fire regulation IFC 605.11.3.3.1, 1.8 m space around the perimeter wall is necessary for buildings larger than 76.2 m to allow firefighters access to the roof [54]. In addition IFC 605.11.3.3.2 and 605.11.3.3.3 require a 1.22 and 2.44 m pathway access [54]. Commercial rooftop solar arrays cannot be greater than 46 by 46 m. Thus, the total roof area available for installation of solar panels was assumed to be 75% of building area [55]. In addition, building's flat roof will typically contain mechanical equipment, such as HVAC, refrigeration, and more.

The Project Sunroof estimated the amount of sun hitting a rooftop using 3D models derived from aerial imagery. The 3D models allowed estimation of shading for every point on a roof, for each possible position of the sun in the sky. The 3D models also enabled the estimation of the amount of available space for solar panels, including the pitch and azimuth of each roof plane. However, the 3D models did not provide data about the available space for solar panels for DC locations used in our models [56].

The Project Sunroof currently covers roughly 60 M buildings in portions of 50 states and Washington DC [56]. The online Project Sunroof tool provided data on energy production from panels placed in the viable roof space, which was calculated based on the typical weather data at the location. A solar installation capacity (kW) was multiplied by the average solar electricity price per kW, which provided the total solar panel cost for each location. Then, a total solar panel cost for each location was divided by total potential of solar electricity at each location. The total potential of solar electricity at each location was equal to a product of sun hours per year, solar potential area available, solar power per area, and DC to AC conversion losses. Wiring losses for DC to AC conversion were 78% [57]. Sun hours per year for each location were obtained from the Project Sunroof [56]. The sum of capital cost and levelized production cost was multiplied by the total electricity purchased (kWh/year) and divided by the DC area (m^2). The solar electricity costs and calculation data and results are provided in the SI, Table S3.

A cost coefficient for wind electricity ($C_{wind(in)}$) was calculated as a sum of wind turbine capital costs and a levelized wind electricity production costs. The capital cost for an on-shore wind turbine was between 1200 and 1650 $/kW and for an off-shore between 2360 and 4500 $/kW. We used average values of 1425 $/kW for the on-shore and 3430 $/kW for the off-shore wind turbine capital costs [51]. Total wind hours were calculated as a ratio of the annual potential electricity generation from wind and the installed wind capacity in each state. The highest on-shore wind energy capital costs was 0.393 $/kWh (Texas) and the highest off-shore wind energy capital costs was 2.36 $/kWh (Virginia). This value was multiplied by the total electricity purchased (kWh/year) and divided by the building area (m^2). The wind energy electricity generation potential and costs calculations are provided in the SI, Table S4.

The minimum non-renewable fossil energy use objective function shown in the Eq. (3) calculated how much of the electricity was purchased from the grid and how much was generated from the on-site solar panels, and nearby wind farms at the lowest total fossil energy used.

$$\underset{x}{min}\ FE_{total} = FE_{mix(in)} \cdot x_1 + FE_{PV(out)} \cdot x_2 + FE_{wind(in)} \cdot x_3, \quad (3)$$

where $\underset{x}{min}\ FE_{total}$ is the total non-renewable fossil energy use. X_1, x_2, and x_3 were variables, which were calculated using the MOO and represent share of grid, solar, and wind energy. $FE_{mix(in)}$, $FE_{PV(out)}$, and $FE_{wind(in)}$ were non-renewable fossil energy coefficients (MJ/m^2) for purchased grid, solar, and wind electricity from the cradle-to-gate LCA, as shown in the SI, Table S1.

The minimum climate change impact objective function is shown in the Eq. (4).

$$\underset{x}{min}\ CC_{total} = CC_{mix(in)} \cdot x_1 + CC_{PV(out)} \cdot x_2 + CC_{wind} \cdot x_3, \quad (4)$$

where $\underset{x}{min}\ CC_{total}$ was the total climate change impact, which showed how much of the purchased grid electricity and electricity generated from on-site solar and nearby wind farm was necessary to buy/produce to obtain the minimal climate change impact. X_1, x_2, and x_3 were variables, which were calculated using the MOO, and represent shares of grid, solar, and wind energy. $CC_{mix(in)}$, $CC_{PV(out)}$, and $CC_{wind(in)}$ were coefficients for climate change impact of grid, solar, and wind electricity from the cradle-to-gate LCA, as shown in the SI, Table S1.

3.2.2. Linear constraints

Bi-optimization and triple-optimization models had the only one linear inequality constraint, i.e. the source energy demand (E_{demand}) for each DC at different locations, as shown in the Eq. (5). The site and source energy for purchased grid electricity for each building were obtained from the EnergyPlus building simulation report [42]. The site to source energy conversion factor depended on the energy mix in electricity generation and varied from 1.74 (Washington) to 3.63

(Texas). A conversion factor for the renewable electricity produced on-site was 1.1.

$$E_{mix\,(in)}\left[\frac{MJ}{m^2}\right]\cdot x_1 + E_{PV\,(out)}\left[\frac{MJ}{m^2}\right]\cdot x_2 + E_{wind\,(in)}\left[\frac{MJ}{m^2}\right]\cdot x_3 \geq E_{demand}, \quad (5)$$

where $E_{mix(in)}$, $E_{PV(out)}$, and $E_{wind(in)}$ were coefficients set to be equal or higher than defined source energy demand (E_{demand}). A source energy demand required by each DC in different locations was obtained from the building energy simulation tool EnergyPlus [42]. The assumption was that there was sufficient source energy from the electricity grid, wind, or solar electricity, and each can be potentially a single source of electricity.

3.2.3. Lower and upper bounds

Lower bounds for a purchased grid, solar, and wind electricity expressed on the basis of the source energy were set to 0, as shown in Eqs. (6), (7), and (8). Upper bounds for purchased grid electricity were 100%, i.e., equal to source energy demand, as shown in the Eq. (6). For solar electricity, upper bounds were chosen to be the maximum available source solar energy at the location, as shown in the Eq. (7). Finally, wind electricity upper bounds were an additional renewable energy necessary to achieve a zero energy building, as shown in the Eq. (8). In case the DCs' solar energy can hypothetically replace 100% of purchased grid electricity, the wind electricity upper bound was set to 0. Calculations of site and source energy potential for solar and wind electricity are shown in the SI, Tables S2, S4, S5, and S6.

$$0 \leq E_{mix\,(in)} \leq E_{demand} \quad (6)$$

$$0 \leq E_{PV\,(out)} \leq \underbrace{E_{PV}}_{max} \quad (7)$$

$$0 \leq E_{wind\,(in)} \leq 100 - \underbrace{E_{PV}}_{max} = \underbrace{E_{wind}}_{max} \quad (8)$$

3.2.4. Goals

The goal attainment problem involves reducing the value objective function in order to attain the goal values given in a goal vector. Thus, instead of minimizing the cost and environmental objectives, we provided a target value for each objective. Target values for optimization were the minimal cost, minimal non-renewable energy, and minimal climate change impact for each location, as shown in the SI, Table S9. The Pareto-optimal solution also depended on the goal value; for example, if the cost of wind energy was lower compared to cost of purchased electricity from the grid, the Pareto-frontier showed a different behavior than whenever the cost of wind energy was higher than purchased from the grid.

3.2.5. Weights

In most real-life problems, defined goals are not achievable. In the goal optimization each objective needs to be weighted. An appropriate set of weights (w_1 and w_2 for bi-objective, and w_1, w_2, w_3 for triple-objective optimization) needed to be defined for each objective. Weights provided a Pareto-optimal set of solutions that reflected the most desirable tradeoffs between the two and three objectives. We defined 50 arbitrary points and weights for the bi-objective optimization and 10 arbitrary points and weights combinations for the triple-optimization model. The weight vectors for the bi-objective and triple-objective optimization were defined in Eqs. (9) and (10), respectively. The number of Pareto-optimal results was ≤50 for the bi-objective and ≤10 for triple-objective optimization. This was because not all solutions were Pareto-optimal. Also, duplicate results may have appeared for multiple weights. Duplicate results for different weights were excluded from charts. Each Pareto-optimal solution represented a mix of purchased grid, solar, and wind energy. The percent values were used to build Pareto LCA models. The assigned DC uncertainty was equal to the baseline. The Pareto LCA models were compared to the baseline LCA model using the Monte Carlo pairwise comparison to find the cost-effective and superior Pareto-optimal solution.

$$\sum_{i=0}^{2} w_i = 1, \quad w_i \geq 0 \quad (9)$$

$$\text{Weight} = [w_{cost}, w_{non\text{-}renewable\ fossil}] = [w_{cost}, w_{climate\ change}]^1$$

$$\sum_{i=0}^{3} w_i = 1, \quad w_i \geq 0 \quad (10)$$

$$\text{Weight} = [w_{cost}, w_{non\text{-}renewable\ fossil}, w_{climate\ change}]^2$$

Bi-optimization and triple-optimization Matlab codes are reported in the SI. Also, Matlab input files were submitted to Mendeley data.

3.3. Life cycle impact assessment method

The non-renewable fossil energy use was calculated using upper heating values of fossil fuel resources. Characterization factors for the non-renewable fossil energy use are reported in the Cumulative Energy Demand (CED) method [58,59]. By definition, the non-renewable fossil energy use includes life cycle direct and indirect fossil energy and energy consumed during the extraction, manufacturing, and disposal of the raw and auxiliary materials. The Intergovernmental Panel on Climate Change (IPCC) climate change global warming potentials with a timeframe of 100 years were used to calculate the climate change impact [60].

3.4. Monte Carlo uncertainty analysis

Relative differences in environmental impacts result between DCs were not enough to support informed decision-making due to uncertainty in LCIA results. Uncertainty in environmental impacts can overpower the relative difference between different DCs. Quantification of uncertainties in LCI input data supports informed decision-making. LCIA results depend on input parameters including LCI input data and characterization factors. Both LCI input data and characterization factors had a degree of uncertainty, which may be due to lack of knowledge regarding input data or due to inherent variability of the data. Both can be described by a probability distribution. Because of uncertainty in input data, there was not a single number to represent the potential environmental impacts of DCs. At present, the uncertainty analysis helps us understand to what extent results of an LCA were affected by uncertainty of input parameters. Uncertainty of characterization factors is not yet implemented in the SimaPro© 8.4 software [46]. Thus, we can only show a distribution of LCA results due to uncertainty of LCI input parameters. A typical method to calculate uncertainty of the LCIA results due to input parameters is the Monte Carlo uncertainty analysis. The Monte Carlo uncertainty analysis randomly samples the input data space.

The LCI of electricity generation in different states in building models originated from the DataSmart database, which was described in our previous work [34,61]. The US-EI database is a modified Ecoinvent v2.2 databases with most European electricity unit processes replaced by the U.S. electricity mix. DataSmart database added state-

[1] [0.02, 0.98; 0.04, 0.96; 0.06, 0.94; 0.08, 0.92; 0.1, 0.9; 0.12, 0.88; 0.14, 0.86; 0.18, 0.82; 0.16, 0.84; 0.2, 0.8; 0.22, 0.78; 0.24, 0.76; 0.26, 0.74; 0.28, 0.72; 0.3, 0.7; 0.32, 0.68; 0.34, 0.66; 0.36, 0.64; 0.38, 0.62; 0.4, 0.6; 0.42, 0.58; 0.44, 0.56; 0.46, 0.54; 0.48, 0.52; 0.5, 0.5; 0.52, 0.48; 0.54, 0.46; 0.56, 0.44; 0.58, 0.42; 0.6, 0.4; 0.62, 0.38; 0.64, 0.36; 0.66, 0.34; 0.68, 0.32; 0.7, 0.3; 0.72, 0.28; 0.74, 0.26; 0.76, 0.24; 0.78, 0.22; 0.8, 0.2; 0.82, 0.18; 0.84, 0.16; 0.86, 0.14; 0.88, 0.12; 0.9, 0.1; 0.92, 0.08; 0.94, 0.06; 0.96, 0.04; 0.98, 0.02].

[2] [0.25,0.25,0.5; 0.25,0.5,0.25; 0.5, 0.25, 0.25; 0.2,0.2,0.6; 0.2,0.6,0.2; 0.6,0.2,0.2; 0.1,0.1,0.8; 0.1,0.8,0.1; 0.8,0.1,0.1].

level electricity production LCA models and uncertainty analysis based on the national statistics and approximation with the Ecoinvent 2 database [61].

For input parameters originated from the EnergyPlus building simulation model [42], the uncertainty was based on previously published work [62]. EnergyPlus building simulations contain 1000 s parameters, which can be a source of uncertainties [62]. Authors studied the influence of 1000 input parameters on output results in EnergyPlus models [42]. The input parameters were varied ± 20% of their modeling value. The research identified which internal or intermediate processes transmitted the most uncertainty to the final output [62]. Authors used a quasi-random sampling approach and a uniform distribution for all nonzero parameters, and an exponential distribution for parameters with zero nominal values [62]. The standard deviations in annual energy consumption (%) were used to calculate minimum and maximum uncertainty values of the LCI input data including HVAC, lighting, equipment, and refrigeration [62]. For those parameters, a uniform distribution was adopted as in Eisenhower et al. (2011) [62].

We calculated a distribution range for other LCI input parameters including conveyor, size of the building, refrigerant loss, and water consumption. For the size of the building and the length of conveyor, we used the range reported for the Walmart Inc. DC network. For the envelope material, the LCI uncertainty was calculated using the guidance on quantitative inventory uncertainty [63]. We kept the shape and orientation of the DC constant in accordance to research published by Eisenhower et al. [62]. The uncertainty values for input LCI parameters are reported in Table 1.

3.5. Monte Carlo pairwise comparison

The scope of this work also included comparative assertions based on (a) the Monte Carlo pairwise comparison between the baseline DC network and (b) the Monte Carlo pairwise comparison between the baseline DC and the Pareto-optimal set of results for the same DC. The Monte Carlo pairwise comparison considered a cradle-to-grave LCA, which accounted for the electricity production uncertainty [61] and the EnergyPlus model uncertainty [62]. Requirements to perform a pairwise Monte Carlo comparison and to provide comparative assertions were fulfilled [65]. Comparative assertions were justifiable because (1) there were no data gaps in models, (2) the choice of environmental categories was appropriate in relation to the goal of the study to reduce fossil energy consumption and climate change impact, (3) modelled data was precise compared to the database, (4) data were complete and representative, (5) LCA models were consistent, (6) input data collected, data treatment, and results were reproducible [44]. These data properties and models guaranteed that the comparison was fair and equivalent for building alternatives.

Table 1
Uncertainty assigned to LCI input data.

LCI input data	Reference	Distribution	Standard deviation (SD^2)
DataSmart			
Electricity mix	National statistics [61]	Lognormal	1.5
Transmission	Ecoinvent 2 [64]	Lognormal	2.0
Solar energy (flat roof panels)	Ecoinvent 2 [64]	Lognormal	1.1
Wind energy (onshore)	Ecoinvent 2 [64]	Lognormal	1.3
Wind energy (offshore)	Ecoinvent 2 [64]	Lognormal	1.3
EnergyPlus			Relative standard deviation (%)
HVAC (GJ)	[62]	Uniform	12%
Electricity (GJ)	[62]	Uniform	7.5%
Heating (GJ)	[62]	Uniform	10%
Interior equipment (GJ)	[62]	Uniform	5.0%
Interior lights (GJ)	[62]	Uniform	6.5%
Cooling (GJ)	[62]	Uniform	22%
Pumps (GJ)	[62]	Uniform	10%
Fans (GJ)	[62]	Uniform	12%
Refrigeration (GJ)	[62]	Uniform	16%
Other			
Conveyor (km)	calculated[1]	Uniform	23%
Conveyor energy use (kWh/km)	assumed	Uniform	20%
Envelope material (kg)	assumed	Uniform	20%
Refrigerant loss (kg)	assumed	Uniform	20%
Water consumption (m^3)	calculated[2]	Uniform	5.7%

[1] Relative standard deviation– standard deviation of the conveyor sample divided by the mean.

[2] Relative standard deviation – standard deviation of the water consumption of walk-in units, cases, and dock divided by the mean.

Because of uncertainty in the LCA models, the building with lower environmental impacts does not guarantee that it is better than the building with higher environmental impacts. In other words, they might not be statistically different due to uncertainty in input data. To prove, (1) that one building in a state is statistically different, i.e., superior, to others in the same state or in different states (baseline to baseline comparison) and (2) that baseline building is statistically different than its alternative solution (baseline to Pareto-optimal solutions comparison); we used the Monte Carlo pairwise comparison.

Each building LCA model had more than 7,000 processes with assigned uncertainties. During the Monte Carlo pairwise comparisons, all processes, typically the background process such as electricity generation, which pairs share, were fixed to the same value. The Monte Carlo pairwise comparison compared all 1 to X times pairs in the baseline to baseline DC comparison or baseline to Pareto-optimal DC comparison under consideration, which enabled a true comparison and finding alternatives that are superior, and thus, considered better from the environmental impact perspective. As a rule of thumb, we chose X to be 1,000 Monte Carlo comparisons. In each Monte Carlo run, the baseline or alternative LCA model had higher or lower environmental impacts. The model counted how many times the baseline building had lower environmental impacts and how many times the other baseline or alternative. If 90% of time out of 100%, the baseline building had higher environmental impacts than alternative, we can say with 90% confidence that the alternative system was superior to the baseline for those impact categories. If the result was less than 90% for either of buildings, we said it was inconclusive or buildings were not different even though one had lower environmental impacts in the LCIA step of the analysis.

3.5.1. The Monte Carlo comparison of GMDCs, PDCs, and GDCs

First, the Monte Carlo pairwise comparison was performed between each pair of the baseline DC network. GMDCs were compared to other GMDCs, GDCs were compared to other GDCs, and PDCs were compared to other PDCs. Thus, the Monte Carlo pairwise comparison was conducted between the baseline whole-building LCA model for one location and the baseline LCA model of the building located in the same state or in a different state. The purpose of the Monte Carlo pairwise comparisons of the baseline DCs was to find DC locations for which reduction in environmental impacts should be a priority. The Monte Carlo pairwise comparison provided information if one DC had a statistically different environmental impact compared to other DCs in the network.

3.5.2. The Monte Carlo comparison of baseline and alternative solutions

The MOO provided 10 to 20 alternative solutions for each building. Relative differences in environmental impacts between the baseline DC and Pareto-optimal alternatives were not enough to support informed decision-making. Monte Carlo pairwise comparisons of the baseline DCs and Pareto-optimal solutions support informed decision-making. Thus, after obtaining the Pareto-optimal solutions for each building, the

baseline DC was compared to Pareto-optimal solutions for the DC to find the closest alternative optimal solution, which was superior to the baseline. This process was iterative until a superior Pareto-optimal solution was found for each DC.

3.6. The good, the better, and the zero DC network

A further analysis of the Pareto-optimal results was necessary to narrow down results to three different DC solutions from the Pareto frontier, which abide to several additional criteria. The better building criterion was an LCA-based criterion for superiority of one building over another and the zero energy criterion was based on the DOE definition. We used the good, the better and the zero energy building criteria to find the best individual DCs and identify tradeoffs of those solutions. Thus, the final results of the bi- and triple-objective optimization were Pareto-optimal solutions obtained by weighting importance of criteria; i.e., from the baseline DC network, the good DC network, the better DC network, to the zero energy DC network.

We developed two new definitions for the good and the better buildings and expanded the definition of the zero energy building. The better DCs were a Pareto-optimal set of buildings, which showed demonstrated superiority compared to the baseline building from the LCA perspective. Pareto-optimal DCs based on bi-objective and triple-objective optimization were compared to the baseline DC starting from the Pareto-optimal solution which yielded the lowest cost to assure that the selected better building was also cost-effective. The single better DC was the first Pareto-optimal DC building that showed superiority in both climate change impact and non-renewable fossil energy use when a Pareto LCA model was compared to a baseline LCA model via Monte Carlo pairwise comparison. The good DCs were characterized by the alternative Pareto-optimal solutions between the baseline and the better building. In some cases, the good building was equal to the baseline.

The term zero energy building has been used for over 20 years, but no common definition had been established. The U.S. Department of Energy (DOE) evaluated current definitions and solicited industry input to formulate a common definition and nomenclature for zero energy buildings [66]. According to the DOE, the zero energy building was defined as an energy-efficient building where, on a source energy basis, the actual annual delivered energy was less than or equal to the on-site renewable exported energy [66]. Different renewable energy combinations can be used to achieve zero energy targets in buildings. However, we were interested in solutions that will have the minimal cost, minimal non-renewable energy, and minimal climate change impact. Thus, we expanded upon the DOE definition and evaluated only zero energy results obtained by the MOO, i.e., the Pareto-optimal zero energy and near zero climate change building.

4. Results and analysis

4.1. The Monte Carlo uncertainty analysis

We used 1,000 Monte Carlo uncertainty runs to calculate environmental impacts' distribution and 95% confidence interval of the LCIA results. Individual box-and-whisker plots in Fig. 3 show Monte Carlo uncertainty results for the baseline cradle-to-grave climate change impact results of GDCs, GMDCs, and PDCs. The box plot shows the first and third quartile also called the 25th and 75th percentile. The thick black line is the mean value. The interval between the upper and lower whisker shows the maximum extent of the Monte Carlo uncertainty results for each DC type.

The size of the box-and-whisker plots was similar across different states and DC type. The mean value in Fig. 3 showed that GDCs, GMDCs, and PDCs, had a different climate change impact. This is because GMDCs, PDCs, and GDCs have different operations. Refrigerated PDCs and GDCs had a higher climate change impact than GMDCs [34]. Within the same type of DCs, mean values varied for the climate change impact [34], as shown in Fig. 3. The state-level differences originated largely in the energy mix used to generate electricity in each state. Other differences were due to different lengths of conveyor, climate zone, and building age [34]. Some DCs showed overlapping or similar range of the climate change impact, for example, GDCs in Bartsville, Oklahoma and Clarksville, Arkansas, others had a different range, for example, the GDC in Grandview, Washington, as shown in Fig. 3.

The primary uncertainty in LCIA results originated from uncertainty in input parameters used in electricity generation and not from the uncertainty originated in EnergyPlus models [42]. The GDC in Washington and the GMDC in Oregon had the lowest impact to climate change, which was linked to (1) 36–70% natural gas and 4% hydropower in electricity generation fuel profile and (2) a lower energy demand due to cold climate zone. The minimum and maximum values (whiskers) for the climate change impact of GDCs and PDCs were 25 and 4554 kg CO_2-eq/m^2, respectively, as shown in Fig. 3a and b. For GMDCs, the range of climate change impact was from 14 to 996 kg CO_2-eq/m^2, as shown in Fig. 3c.

4.2. The Monte Carlo pairwise comparison

The Monte Carlo uncertainty results were not enough to make a comparative assertion about the superiority of the GDC in Grandview, Washington. The Monte Carlo pairwise comparison was needed to reaffirm that Grandview, Washington was statistically different, and thus, superior to other GDCs. The results of Monte Carlo pairwise comparisons for the climate change impact category are shown in Tables 2 and 3. The results of Monte Carlo comparisons proved or dismissed differences in the climate change impact observed in Fig. 3. Also, it identified buildings that perform worse than others in the network and needed to be improved first. We choose only one impact category because reducing climate change impact will reduce other environmental impacts.

All DCs in rows (A) were compared to DCs in the columns (B), as shown in Tables 2 and 3. The result of each Monte Carlo comparison was reported in non-diagonal boxes. If the DC A had 90% out of 1,000 runs of the time a lower LCIA result than the DC B, then DC A was superior to DC B. If the DC A had 90% out of 1,000 runs of the time higher LCIA result than DC B, then the DC A was inferior to the DC B, as shown in Tables 2 and 3. The Monte Carlo comparison of the GDC in Brundidge, Alabama was statistically different and had a lower climate change impact compared to the GDC in Park Way, Indiana, which was highlighted by a green color and annotated with the less than (<) symbol in the Table 2. Also, the GDC in Brundidge, Alabama was statistically different and had a higher climate change impact compared to the GDC in Grandview, Washington, which was highlighted by the red color and annotated with the greater than (>) symbol.

A summary of pairwise comparisons was given in diagonal squares. Squares' color and symbols showed whether a DC in the row A was superior, inferior or equal to a DC in the column B. The green square and less than (<) symbol meant that the climate change impact of the DC in the row A was 90% of time less than impact of the DC in the column B. The red square and greater than (>) symbol meant that the climate change impact of the DC in the row A was 90% of the time higher than the impact of the DC in the column B. Orange squares and = symbols meant that the impact of the DC in the row A was not statistically different from the DC in the column B. Colored diagonal squares showed the dominant and conclusive characteristic (superior, inferior, and equal) of the DC in the row A. Numbers in black framed squares showed how many times the DC in the row A was superior, inferior or both compared to the DC in the column B.

The results of Monte Carlo pairwise comparison of baseline DCs in different states proved with the 90% confidence that the GDC in Washington was superior to other GDCs and the GMDC in Oregon was superior to other GMDCs, as shown in Table 2 and Table 3, respectively. The GDC in Indiana had statistically higher impact compared to GDCs

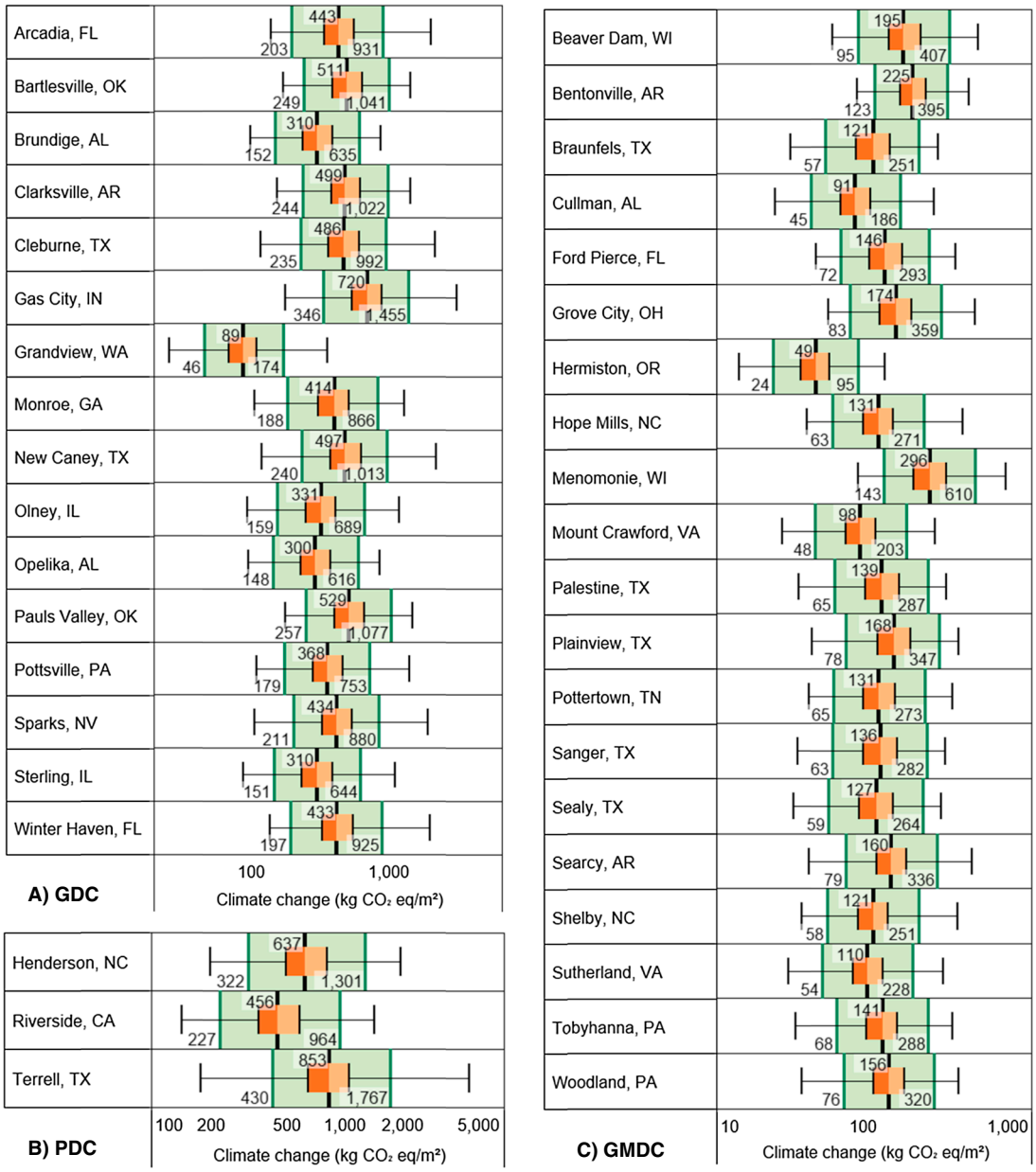

Fig. 3. Box-and-whisker plot cradle-to-grave LCIA results uncertainty analysis results for baseline (A) GDCs, (B) GMDCs, and (C) PDCs, based on distribution range in Table 1. A thick black line is the mean value. Lower and upper whiskers are the maximum extent of the Monte Carlo results. The green area is the width of the 95% confidence interval bounded by the 5th (2.5%) and 95th (97.5%) percentile. The box plot shows the first and third quartile also called the 25th (dark orange) and 75th percentile (light orange). The x-axis is in logarithmic scale. (For interpretation of the references to colour in this figure legend, the reader is referred to the web version of this article.)

in Alabama, Pennsylvania, Illinois, and Washington. The PDC in California was superior compared to the PDC in Missouri. Arkansas, Ohio, and Wisconsin. In Texas, the GMDC in Plainview was inferior to GMDCs in Braunfels and Sealy. Other results were inconclusive, i.e., the LCIA impact of the DC A was not statistically different from the DC B, as shown by the prevalence of orange and = symbol squares. Thus, primary efforts to reduce the climate change impact should focus on DC locations in Arkansas, Indiana, Ohio, and Wisconsin.

4.3. The good, the better, and the zero energy distribution center network

Pareto-optimal sets were results obtained by weighting objectives' importance. Summary results of bi-objective and triple-objective optimization were presented in the 2D Pareto front chart in Fig. 4. A Pareto front was annotated with the arrow going through the center of a pie, as shown in the Fig. 4a. The size of the pie did not show any particular metric in the Fig. 4. One pie was highlighted with a diameter bigger than other pies to show the first Pareto-optimal solution for which the improved building was better than the baseline. This was the better DC, which has combined properties of a Pareto-optimality and LCA-based Monte Carlo superiority. All subsequent pies to the right are also better, but the highlighted one has also the lowest cost, as shown in Fig. 4a. The x-axis shows costs ($/m^2) of each Pareto-optimal solution, and the y-axis shows climate change impact (CO_2-eq/m^2). The bi-objective (cost and non-renewable fossil energy use) optimization and triple-objective (cost, non-renewable fossil energy, and climate change) optimization results were plotted in the bi-objective (cost climate change impact) chart due to results similarity, as shown, in Fig. 4. However, the bi-objective cost and non-renewable optimization results and triple-objective optimization results were less dense than the bi-objective cost

Table 2
LCA-based Monte Carlo pairwise comparison between baseline GDCs in different states.

GDCs A - rows B - columns	Brundidge, AL	Opelika, AL	Clarksville, AR	Arcadia, FL	Winter Haven, FL	Monroe, GA	Olney, IL	Sterling IL	Gas City, IN	Sparks, NV	Bartlesville, OK	Pauls Valley, OK	Pottsville, PA	Cleburne, TX	New Caney, TX	Grandview, WA
Brundidge, AL	1/1	=	=	=	=	=	=	=	<	=	=	=	=	=	=	>
Opelika, AL	=	1/1	=	=	=	=	=	=	<	=	=	=	=	=	=	>
Clarksville, AR	=	=	1	=	=	=	=	=	=	=	=	=	=	=	=	>
Arcadia, FL	=	=	=	1	=	=	=	=	=	=	=	=	=	=	=	>
Winter Haven, FL	=	=	=	=	1	=	=	=	=	=	=	=	=	=	=	>
Monroe, GA	=	=	=	=	=	1	=	=	=	=	=	=	=	=	=	>
Olney, IL	=	=	=	=	=	=	1/1	=	<	=	=	=	=	=	=	>
Sterling IL	=	=	=	=	=	=	=	1/1	<	=	=	=	=	=	=	>
Gas City, IN	>	>	=	=	=	=	>	>	6	=	=	=	>	=	=	>
Sparks, NV	=	=	=	=	=	=	=	=	=	1	=	=	=	=	=	>
Bartlesville, OK	=	=	=	=	=	=	=	=	=	=	1	=	=	=	=	>
Pauls Valley, OK	=	=	=	=	=	=	=	=	=	=	=	1	=	=	=	>
Pottsville, PA	=	=	=	=	=	=	=	=	<	=	=	=	1/1	=	=	>
Cleburne, TX	=	=	=	=	=	=	=	=	=	=	=	=	=	1	=	>
New Caney, TX	=	=	=	=	=	=	=	=	=	=	=	=	=	=	1	>
Grandview, WA	<	<	<	<	<	<	<	<	<	<	<	<	<	<	<	15

< A has statistically significant lower impact than B in climate change impact category. More than 90% of the time A result has a lower impact than B. Thus, A is superior to B
>A has statistically significant higher impact than B in climate change impact category. More than 90% of time A result has higher climate change impact than B. Thus, A is inferior compared to B.
= Inconclusive. A is not environmentally superior to B in climate change impact category.
Color legend: red – inferior, yellow – equal/inconclusive, and green – superior.
Numbers in diagonals show how many times certain building is superior (green) and inferior (red), mostly superior (green/red), equal (yellow) to other buildings.

and climate change impact results (i.e., the number of Pareto-optimal results was lower than for bi-objective cost and climate change optimization), as shown in the SI, Figures S10 and S11. Numerical results for the individual bi-optimization (cost and non-renewable fossil energy and cost and climate change) and the triple-optimization (cost, non-renewable fossil energy, and climate change) are shown in the SI, Excel document "2_Pareto front numerical results.xlsx".

Pie slices show shares of energy sources (purchased grid, solar, and wind) for different objectives' weighting combinations, which satisfy the energy demand of DCs in different locations. The baseline solution in most cases was an optimal result for a single-objective optimization with 100% purchased grid electricity, in which the objective was only to minimize cost. For several locations including Brundidge (AL), Clarksville (AR), Riverside (CA), Winter Haven (FL), Sterling (IL), Olney (IL), Gas City (IN), Grove City (OH), Bartlesville (OK), Pottsville (PA), Woodland (PA), Tobyhanna (PA), Terrell (TX), and Menomonie (WI), the baseline solution was not a part of the optimal result because the purchased grid electricity ($/m^2) had a higher cost than the purchased off-site wind electricity, as shown in the SI, Table S1. Thus, baseline solutions were added to the Pareto-optimal results in Fig. 4b, d.

The last pie to the right is the Pareto-optimal result for zero energy DC, as shown in Fig. 4a. All pies between the better DC and the zero energy DC had properties of the better DC, but the solution was more expensive, as shown in Fig. 4a. Finally, because of the better DC definition, another set of DCs were the good DCs, which were Pareto-optimal cost-effective solutions, but which were not superior compared to the baseline DC, as shown in Fig. 3a. Thus, the environmental performance and energy reduction achieved was not statistically different than the baseline building.

Results in Fig. 4a–d were for a single DC as annotated in the figure title, but similar Pareto-results were found for multiple buildings, and thus, this result was representative for multiple buildings annotated as Group 1, Group 2, Group 3, and Group 4. Individual Pareto-front results for DCs are reported in the SI, Figs. S1–S9. Results in Fig. 5a–d are for single DCs.

Group 1 showed a uniform distribution of Pareto-optimal results for

Table 3
LCA-based Monte Carlo pairwise comparison between baseline GMDCs in different states.

GMDCs A - rows B - columns	Cullman, AL	Bentonville, AR	Searcy, AR	Ford Pierce, FL	Shelby, NC	Hope Mills, NC	Grove City, OH	Hermiston, OR	Woodland, PA	Tobyhanna, PA	Pottertown, TN	Braunfels, TX	Palestine, TX	Plainview, TX	Sanger, TX	Sealy, TX	Mount Crawford, VA	Sutherland, VA	Beaver Dam, WI	Menomonie, WI
Cullman, AL	4/1	<	=	=	=	=	<	>	=	=	=	=	=	=	=	=	=	=	<	<
Bentonville, AR	>	6	=	=	>	=	=	>	=	=	=	>	=	=	=	=	>	>	=	=
Searcy, AR	=	=	1	=	=	=	=	>	=	=	=	=	=	=	=	=	=	=	=	=
Ford Pierce, FL	=	=	=	1/1	=	=	=	>	=	=	=	=	=	=	=	=	=	=	=	<
Shelby, NC	=	<	=	=	2/1	=	=	>	=	=	=	=	=	=	=	=	=	=	=	<
Hope Mills, NC	=	=	=	=	=	1/1	=	>	=	=	=	=	=	=	=	=	=	=	=	<
Grove City, OH	>	=	=	=	=	=	2	>	=	=	=	=	=	=	=	=	=	=	=	=
Hermiston, OR	<	<	<	<	<	<	<	19	<	<	<	<	<	<	<	<	<	<	<	<
Woodland, PA	=	=	=	=	=	=	=	>	1	=	=	=	=	=	=	=	=	=	=	=
Tobyhanna, PA	=	=	=	=	=	=	=	>	=	1/1	=	=	=	=	=	=	=	=	=	<
Pottertown, TN	=	=	=	=	=	=	=	>	=	=	1/1	=	=	=	=	=	=	=	=	<
Braunfels, TX	=	<	=	=	=	=	=	>	=	=	=	3/1	=	<	=	=	=	=	=	<
Palestine, TX	=	=	=	=	=	=	=	>	=	=	=	=	1/1	=	=	=	=	=	=	<
Plainview, TX	=	=	=	=	=	=	=	>	=	=	=	>	=	3	=	>	=	=	=	=
Sanger, TX	=	=	=	=	=	=	=	>	=	=	=	=	=	=	1/1	=	=	=	=	<
Sealy, TX	=	=	=	=	=	=	=	>	=	=	=	=	=	<	=	2/1	=	=	=	<
Mount Crawford, VA	=	<	=	=	=	=	=	>	=	=	=	=	=	=	=	=	3/1	=	<	<
Sutherland, VA	=	<	=	=	=	=	=	>	=	=	=	=	=	=	=	=	=	2/1	=	<
Beaver Dam, WI	>	=	=	=	=	=	=	>	=	=	=	=	=	=	=	=	>	=	3/1	<
Menomonie, WI	>	=	=	>	>	>	=	>	=	>	>	>	>	=	>	>	>	>	>	14

< A has statistically significant lower impact than B in climate change impact category. More than 90% of the time A result has a lower impact than B. Thus, A is superior to B
>A has statistically significant higher impact than B in climate change impact category. More than 90% of time A result has higher climate change impact than B. Thus, A is inferior compared to B.
= Inconclusive. A is not environmentally superior to B in climate change impact category.
Color legend: red – inferior, yellow – equal/inconclusive, and green – superior.
Numbers in diagonals show how many times certain building is superior (green) and inferior (red), mostly superior (green/red), equal

cost and climate change impact optimization. The results for the triple-objective optimization started at a cost value higher than 177 $/m^2 and overlapped with results of the bi-objective optimization. This was due to a result gap for the cost range starting from 110$/m^2 to 130$/m^2, for which the non-renewable fossil energy criteria was not calculated. Single results for Opelika (AL), Monroe (GA), New Caney (TX), Cleburne (TX), and Pauls Valley (OK) of Group 1 are shown in the SI, Figs. S1 and S2. Numerical results are presented in the SI, Excel document "2_Pareto front numerical results.xlsx".

The highlighted pie in Group 1 shows the better DC result. The better DCs in Group 1 was achieved by purchasing 25–37% of off-site wind energy from the nearest location. The Pareto-optimal zero energy DCs included more than 86% wind energy and 14% solar, which was at the maximal solar energy potential that GDCs in Group 1 can produce via on-site roof panels. Arcadia (FL) GMD had a similar Pareto-pies distribution and an equal zero DC profile to Group 1, but a better building included 10% solar and 13% wind energy, as shown in Fig. 5a. For Sparks (NV), Grandview (WA), and Henderson (NC) same conclusions were valid as for Group 1, but the Pareto-front distribution was steeper than for DCs in Group 1, as shown in the SI, Figs. S1 and S2.

In Group 2, all GDCs and PDCs locations had a lower wind energy cost than the purchased grid electricity. Thus, the Pareto-optimal better

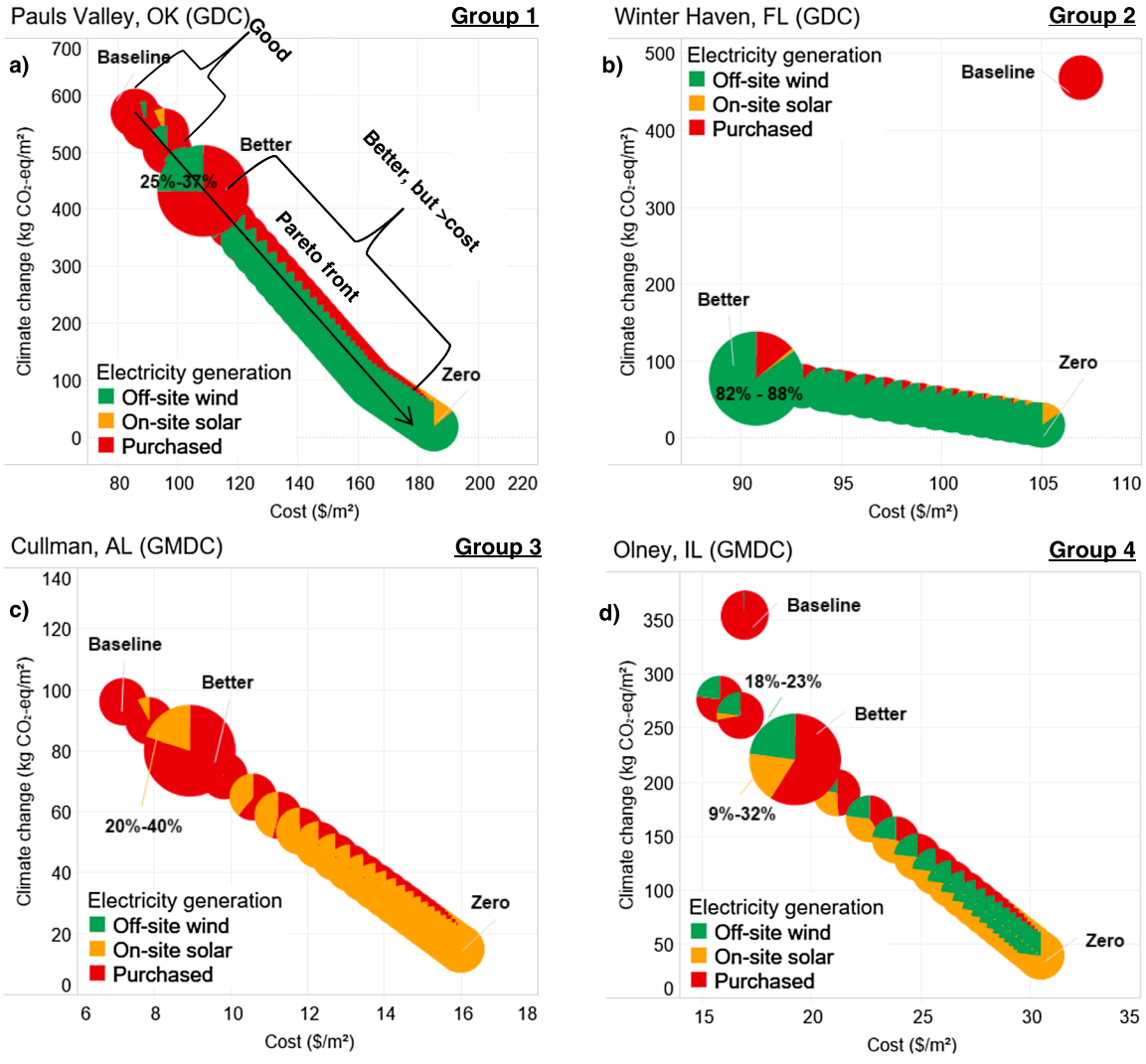

Group1: GDCs in Opelika (AL), Arcadia (FL), Monroe (GA), Sparks (NV), Pauls Valley (OK), New Caney (TX), Cleburne (TX), and Grandview (WA) and a PDC in Henderson (NC).
Group 2: GDCs in Brundidge (AL), Clarksville (AR), Winter Haven (FL), Sterling (IL), Gas City (IN), Henderson (NC), Sparks (NV), Bartlesville (OK), Pottsville (PA), and Grandview (WA) and PDCs in Riverside (CA) and Terrell (TX)
Group 3: GMDCs in Bentonville (AR), Cullman (AL), Searcy (AR), Fort Pierce (FL), Hope Mills (NC), Mount Crawford (VA), Sutherland (VA), New Braunfels (TX), Palestine (TX), Plainview (TX), Shelby (TX), Sanger (TX), Sealy (TX), Beaver Dam (WI)
Group 4: Olney (IL), Grove City (OH), and Tobyhanna (PA), Woodland (PA)

Fig. 4. Combined bi-objective and triple-objective optimization Pareto-optimal results for GDCs, PDCs, and GMDCs. The 2-objective optimization included cost ($/m^2) on x-axis and climate change impact (kg CO_2-eq/m^2) on y-axis. The 3-objective optimization included cost ($/m^2), climate change impact (kg CO_2-eq/m^2), and non-renewable fossil energy ($MJ_{deprived}$/m^2), but is plotted as a projection in a 2D cost-climate change chart. Highlighted pies are Pareto-optimal better DCs results. The last pies on the right are Pareto-optimal zero energy DCs.

DC was also the lowest cost option in which 82–88% electricity was supplied by wind farms. The zero energy DCs had a maximal available energy from solar panels and remaining energy from wind. For GDCs in Winter Haven (FL), Sterling (IL), and Gas City (IN), and PDC in Riverside (CA), the Pareto-optimal zero energy solution had a lower cost compared to the baseline. Individual results for GDCs and PDCs are shown in the SI, Tables S3 and S4.

All solutions for GMDCs in Group 3 produced enough electricity from solar panels to become zero energy DCs. The zero energy DC solution assumed between 64% and 93% of solar energy installation capacity. If maximum solar capacity was installed, GMDCs in Group 3 could export between 7.2% (Cullman, AL) and 92% (Searcy, AR) electricity to the energy grid, which would reduce the cost of the zero energy DC. The better DCs must have at least 20% (Cullman, AL) up to 40% (Bentonville, AR) energy coming from solar panels. Individual results are provided in the SI, Figs. S5 and S6. The GMDC in Midway (TN) had an equal zero energy DC profile compared to the Group 3 (i.e., 100% energy was from solar panels). However, the better building in Midway (TN) required only 5% energy from solar panels, as shown in Fig. 5d.

GMDCs in Group 4 did not produce enough solar energy to reach the zero energy building. All solar energy potential will be used; and thus, for these buildings solar energy storage is not necessary. The better DCs had between 5% (Woodland, PA) and 32% (Grove City, Ohio) of the on-site solar energy production and from 18% (Tobyhanna, PA) to 23% (Olney, IL) of off-site wind energy, which resulted in $1 to $2 increase in cost, as shown in the SI, Fig. S7. The zero energy DCs had between 77% and 82% electricity produced from the maximum potential energy from solar panels and the remaining electricity was supplied by wind farms. The better GMDC at Menomonie (WI) required more than 50% renewable energy, i.e., 47% from wind and 6% from solar energy. The maximum solar energy potential was higher than 50% of the total

source energy demand, and thus, the zero energy building had solar energy at the maximum value. The better GMDC in Hermiston (OR) had 32% energy supplied by solar panels and 6% by wind. Again, the zero energy DC profile was equal to the maximum solar energy potential of 94%, as shown in Fig. 5c.

4.4. Tradeoff analysis of the better, and the zero energy distribution center network

In the tradeoff analysis, we focused only on the three Pareto-optimal solutions: the good, the better, and the zero DC network. First, we analyzed tradeoffs between (1) climate change impact reductions achieved by introduction of solar and wind energy and (2) total energy cost, as shown in Fig. 6a–f.

A summary of climate change impact results for each state (kg CO_2-eq/state) is presented in gradient choropleth geographical map, on top of which we showed results for each location in circles (kg CO_2-eq/m^2), as shown in Fig. 6. The combination chart was named choropie because of pie symbol. A summary of energy costs for each state ($/state) is presented in gradient choropleth geographical map, on top of which we showed relative results for each location using circles and numerical annotations ($/$m^2$), as shown in Fig. 6. The combination chart was named chorobag because of bag symbol.

Fig. 6a shows a baseline result for Walmart Inc. DC network. Fig. 6b and c show a state-level and individual DC's reductions in climate change impact for two Pareto-optimal networks: the better, and the zero DC network. The pies in Fig. 6b and c show relative increase in renewable energy for each scenario, and the circle size shows relative reductions in climate change impact. Overall, the state-level climate change impact was reduced from the baseline to the zero energy networks, while energy costs in most locations increased and in some decreased.

The better DC network showed an increase in wind and solar energy, reaching the maximum of 40% solar energy (GMDC in Arkansas) and between 30% and 90% wind energy, as shown in Fig. 6b. Costs of DCs that were adversely affected by an increase of renewable energy were in Texas, North Carolina, and Florida, as shown in Fig. 6e. DCs' locations where the cost decreased due to introduction of renewable energy were for (1) GDCs in Alabama, Arkansas, Florida, Indiana, (2) GMDC in Wisconsin, and (3) PDC in California and Texas, as shown in

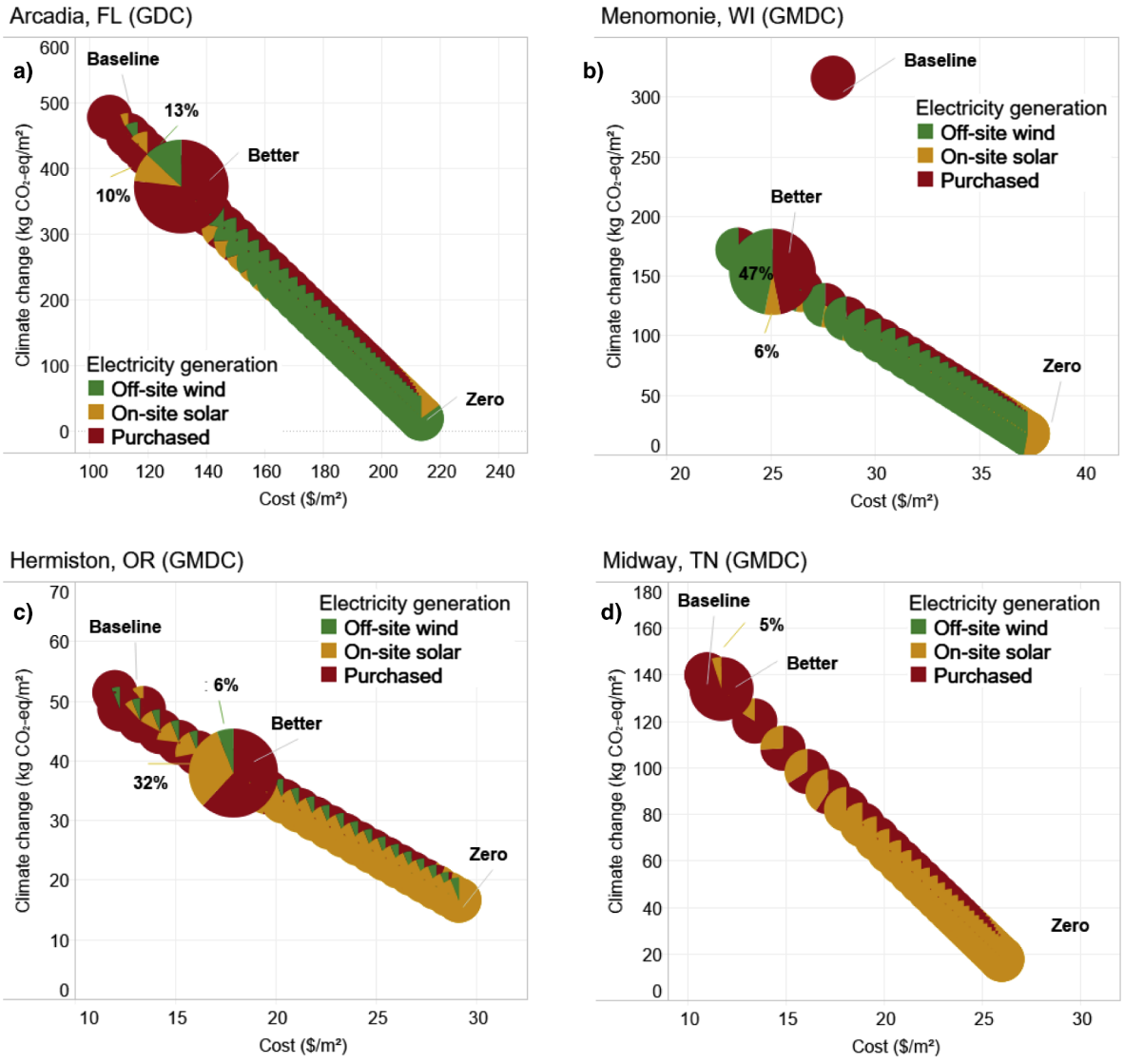

Fig. 5. Combined bi-objective and triple-objective optimization Pareto-optimal results for GDCs, PDCs, and GMDCs. The 2-objective optimization included cost ($/$m^2$) on x-axis and climate change impact (kg CO_2-eq/m^2) on y-axis. The 3-objective optimization included cost ($/$m^2$), climate change impact (kg CO_2-eq/m^2), and non-renewable fossil energy ($MJ_{deprived}/m^2$), but is plotted as a projection in a 2D cost-climate change chart. Highlighted pies are Pareto-optimal better DCs results. The last pies on the right are Pareto-optimal zero energy DCs.

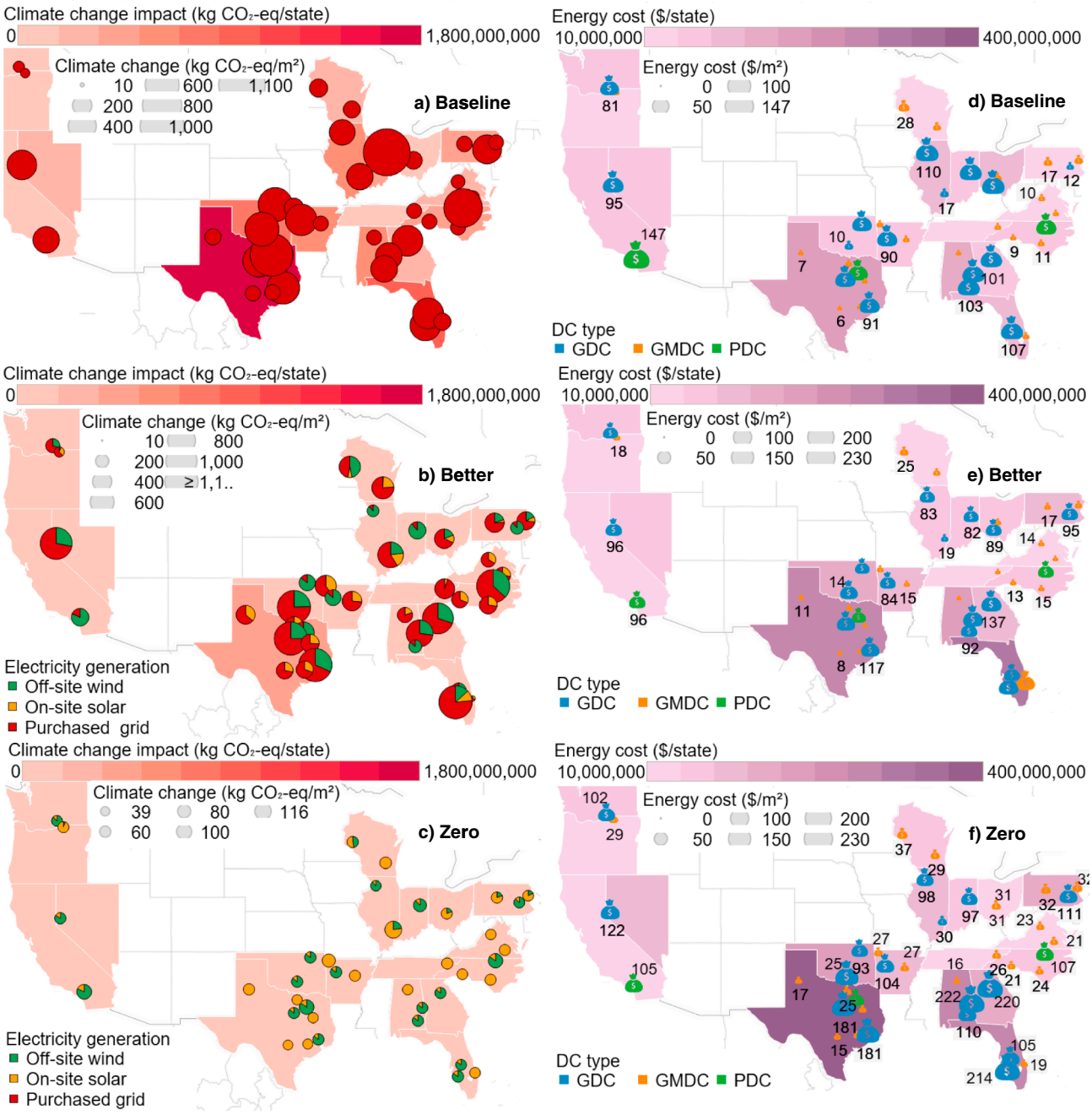

Fig. 6. Choropie plots for the baseline, the better and the zero energy DC network. The size of the pies shows the DCs' climate change impact for each scenario ($/m^2). The multi-color pies show a share of purchased grid, on-site solar, and off-site wind energy in the better and the zero solutions. Choropleth maps with gradient color show combined climate change impact of all DCs in one state (kg CO_2-eq/state). Chorobag plots shows cost tradeoffs in the (f) better, and (g) zero energy DCs compared to (e) baseline due to increase of renewable energy. Dollar bag color shows DC type. Symbol size shows relative magnitude of total energy cost per area ($/m^2). Annotations below show individual DC's cost ($/m^2). Graduated choropleth maps show relative cost for all buildings in one state ($/state). (For interpretation of the references to colour in this figure legend, the reader is referred to the web version of this article.)

Fig. 6e. The range of decrease in cost was between 6.5% (GDC in Arkansas) and 34.4% (PDC in California). The average cost increase was 27.3%. The minimal cost increase of 1.4% was observed for a GDC in Nevada and maximum 91% for a GMDC in Florida.

Zero energy DCs had fivefold lower climate change impact compared to the baseline, as shown in the graduated choropleth shades in Fig. 6c. The size of the circle in the zero energy DC network solution shows the minimal climate change impact, which is not equal to zero because it includes construction material and renewable energy infrastructure and energy production burdens. Despite the 3–4 times higher energy demand for PDCs and GDCs compared to GMDCs, and statistically proven differences between their climate change impact (Fig. 6a), in the zero energy DC solutions the climate change impact results fell within the narrow range for all buildings, as shown in Fig. 6c. In the zero energy solution, most GMDCs had only solar energy, because solar energy potential was sufficient to replace purchased grid energy. The reduction in climate change impact for GMDCs that served as energy producers and performed at the zero energy DC solar energy capacity may be higher if we installed the maximum number of panels and exported solar energy. However, this research was limited to attributing

and satisfying energy demand for the given network and omitting the consequences of the solar energy export. Numerical results are reported in the SI, Excel document "3_Numerical results for the good the better and the zero DCs.xlxs".

The majority of the zero energy DCs showed relative increase in costs compared to the baseline, as shown in Fig. 6f. On average, the zero energy buildings increased their costs by 44.7%. The minimum cost increase was for the zero energy PDC in Terrel, Texas (2.4%), and the maximum was for the two GMDCs in Searcy and Bentonville, Arkansas (63%). The highest reduction in costs was found for the PDC in California 28% compared to the baseline. Only three other locations showed a reduction in the building energy costs due to the cheaper wind energy including GDCs in Gas City, Indiana by 7%, Sterling, Illinois by 13%, and Winter Haven, Florida by 2%. At those locations, the absence of solar energy suggests a cost-effective zero energy building. Based on these results, the best candidates for zero energy buildings were (1) GDCs that showed a cost decrease due to cheaper wind energy and (2) GDCs and PDCs with a maximum of 10% increase in cost, such as Brundidge (AL), Bartlesville (OK), and Terrell (TX). Numerical results are presented in the SI, Excel document "3_Numerical results for the good the better and the zero DCs.xlxs".

4.5. Wind turbine and solar panel capacity needed to achieve the better, and the zero energy scenarios

Geographical maps with a wind turbine symbol (chorowind) and annotation present the number of wind turbines necessary for the whole building to achieve the better and the zero energy DC scenarios, as shown in Fig. 7a and b. Annotations below the number of wind turbines show installation capacities (2 MW, 4 MW, 14 MW, and 16 MW) specific to each location. Third annotation shows a power curve for onshore wind turbines and offshore wind farms. The power curve is the steady power delivered by the turbine as a function of steady wind speed between the cut-in and cut-out speeds. Installation capacities, power curve, choice of onshore and offshore wind farms were based on the National Renewable Energy Laboratory (NREL) recommendations for current and near future wind farms, which were the closest to DC locations [67]. For most wind farm locations, the NREL assumed 16 MW wind turbines. The size of wind turbines affected the number of wind turbines necessary. PDCs and GDCs needed between 2 and 7 of 16 MW wind turbines for the better building scenario, and up to 8 of 16 MW wind turbines for the zero energy. The choropleth map gradient color shows the total electricity produced from wind energy in each state. Under the zero energy scenarios, Florida, Texas, and Alabama produced the highest amount of wind energy, as shown in Fig. 7b.

Geographical maps with a solar panel symbols (chorosolar) show solar panel installation power for each location and building type for better and zero energy scenarios, as shown in Fig. 7c and d. Second annotations show the total solar panel area estimated for better and zero energy scenarios. PDCs are the most energy intensive buildings because all sections are using refrigeration. For PDCs located in California, North Carolina, and Texas the better PDC scenario did not have solar energy in the energy mix because wind energy was cheaper in those locations. GMDCs have more potential for solar energy. This is

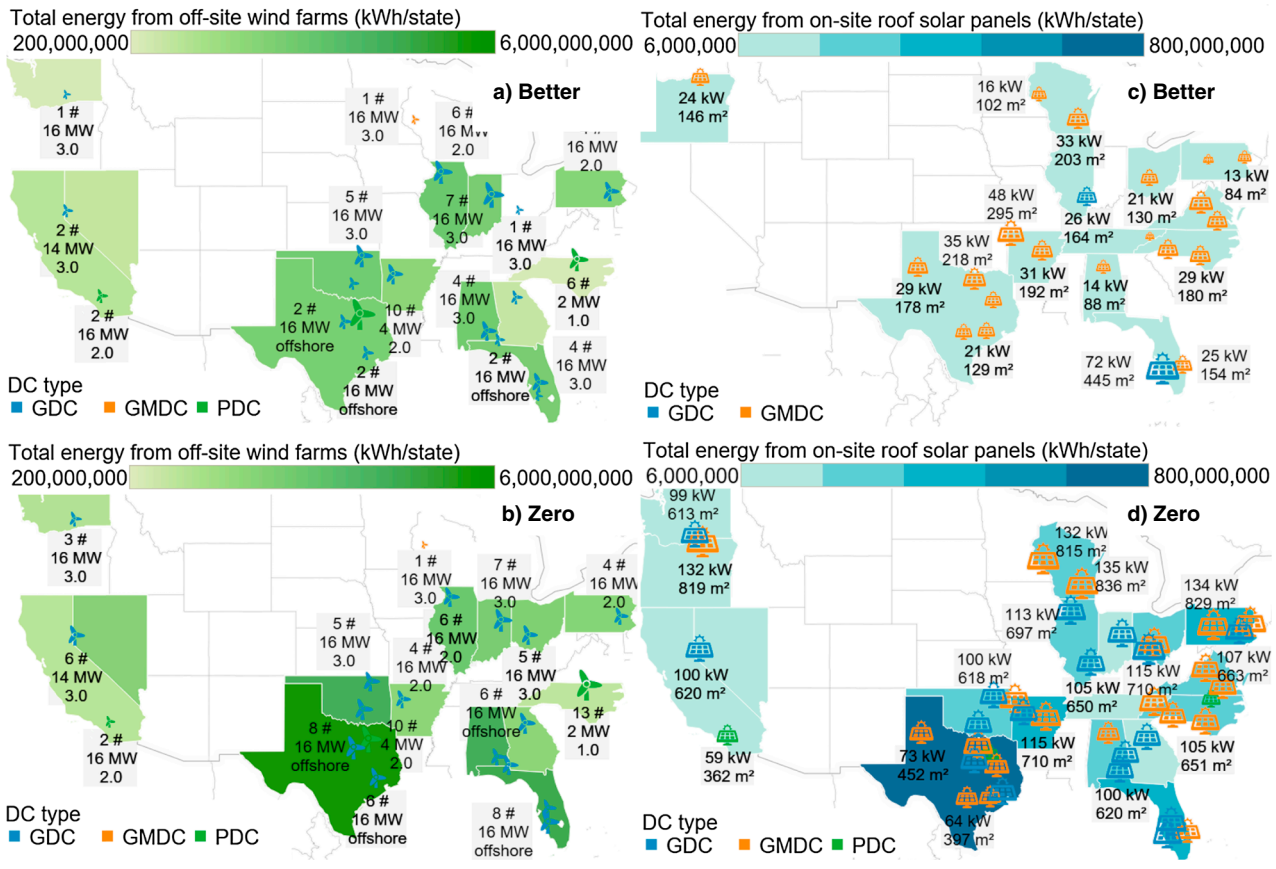

Fig. 7. Chorowind – a geographical map with a wind turbine symbol shows number of wind turbines that need to be installed for (a) better DCs and (b) zero energy DCs. Numerical values are annotated to each wind turbine. Wind turbine color shows DC type. Wind turbine size shows how many wind turbines is necessary to install for (a) better DCs and (b) zero energy DCs. Graduated choropleth maps show state-level wind electricity generation (kWh/state). Chorosolar – a geographical map with a solar panel symbol shows kW of solar panels that need to be installed for (c) better DCs and (d) zero energy DCs. Numerical values for kW installed and total solar panel area (m^2) are annotated for each solar panel. Solar panel color shows DC type. Graduated choropleth maps show state-level solar electricity generation (kWh/state).

true, in particular for GMDCs that can produce enough energy from solar panels to satisfy electricity and even more so for GMDCs that can potentially produce more electricity than needed and export it to the electricity grid. GMDCs that can export solar electricity are: Cullman, Alabama, Searcy, Arkansas, Bentonville, Arkansas, Fort Pierce, Florida, Gas City, Indiana, Hope Mills, North Carolina, Shelby, North Carolina, Pottertown, Tennessee, Palestine, Plain View, Sanger, and New Braunfels in Texas, and Mount Crawford and Sutherland, Virginia. Their potential depended on the energy demand and of solar days. The range of electricity produced beyond the building demand was estimated between 134 MJ/m^2 (Searcy, Arkansas) and 2,242 MJ/m^2 (Sealy, Texas), in other words, each building can produce 10% and up to 2.3 times more energy than required. Numerical results are presented in the SI, Excel document "3_Numerical results for the good the better and the zero DCs.xlxs".

4.6. Discussion of applications and broader impact

In an effort to identify reduction opportunities from electric grid dependency of buildings, this study analyzed the replacement of fossil-fuel derived electricity with an optimal combination of wind and solar energy. Renewable energy sources were shown to be beneficial in building sustainability in certain locations. However, a solution that worked for one location did not work for other locations in terms of wind-to-solar energy ratio and their cost-effectiveness.

The discussion presented here may have important implications to environmental policy and building energy codes. Decision-makers set targets based on percent reductions, which do not guarantee that the building is better than the existing due to underlying uncertainties, as we showed in this research. In practice, the environmental impact reduction targets and criteria about the environmental impact and cost importance were historically based on expert judgment [68]. The predefined importance criteria may fail in reducing enough the environmental impacts to show a statistically better improvement from the baseline. Also, the importance of criteria may be different for different locations. For example, the policy maker may choose to give a climate change impact a relative importance of 30%. However, results have shown that for a non-refrigerated distribution center it is enough to have the climate change criteria set to 10% to achieve a better building. For the non-refrigerated distribution centers, the cost and climate change impact should have equal importance if we wanted to achieve the zero energy building. For refrigerated buildings, the relative importance of the climate change criteria should be around 50%, but to achieve the zero energy, it should be 80%. By using the results of this research, policy makers can make a more informed selection of the importance of criteria to achieve substantial improvements.

Furthermore, the results presented here may be applicable to other buildings, for example, buildings located in Arkansas, Indiana, Ohio, and Wisconsin performed worse and could become vulnerable first with policies to reduce fossil energy use. It is important to note that the uncertainty analysis provided additional confidence in the results and conclusions. The Monte Carlo pairwise comparison is frequently overlooked in the LCA research. According to ISO, differences in life cycle impact results are not sufficient to make comparative assertions about superiority of one system over another.

A barrier to implementing renewable energy was a higher cost of the zero energy distribution centers network compared to the baseline. The cost increase was from 1 to 11 times for the zero energy distribution centers. Thus, the best candidates for the zero energy distribution centers were Brundidge (AL), Bartlesville (OK), and Terrell (TX) with a cost increase of 10% or less. The MOO pointed to cost savings in implementing renewable energy when potential wind energy was cheaper in some locations. We identified a number of distribution centers which showed cost reduction for the zero energy building network including Gas City (IN), Sterling (IL), Winter Haven (FL), and Riverside (CA), whereas some general merchandise distribution centers showed potential to become solar energy producers and exporters.

The study put forward an alternative, more precise definition of the zero energy buildings – that a zero energy building is a cost-effective life cycle assessment-based Pareto-optimal solution, which at the same time maximizes the on-site solar energy production. This underlined the importance that a building should neither depend on the available renewable energy at nearby locations nor depend solely on the on-site energy production. In addition, the study provided two additional definitions, i.e., of the good and the better building. The better building is an intermediate, but the most feasible cost-effective and more sustainable solution, at present. The good building is a feasible, least-costly solution in cases where the increase in cost for the better building is too high.

Also, the variety of solutions underlines the importance of including location specific characteristics such as purchased grid and renewable energy costs, building energy demand, climate zone, electricity grid, solar production potential, and wind potential. The reductions presented here will have positive implications to food distribution sustainability. Because of location specific solutions, the research presented here may be of practical importance in further sustainable distribution center location decision-making and reducing food storage impact. However, other factors and possible tradeoffs need to be considered, such as food-miles, i.e., a new location needs to be such so that will not increase other food environmental impact.

One application of this research is incorporating results into traditional mathematical procedures for selecting new DCs locations, which will include information about food market areas, location cost, zero energy, and minimal environmental impact of building. The models and procedures used in this study can also be applied to other types of buildings available in the EnergyPlus [42].

5. Conclusions

Reducing energy consumption and anthropogenic environmental impacts of buildings is a costly and complex challenge. Businesses' decision-making about reducing energy consumption in commercial buildings is typically based on costs. However, the consequences of a change in building and energy systems are mainly unknown and difficult to predict, for example, a reduction in climate change impacts may increase costs, as shown in this study. This study represents a first attempt at reducing the environmental impacts of a large scale multi-facility distribution center network by installing solar and wind energy systems at minimal costs. Also, the study provides a holistic view about the potential of cost-effective implementation of solar energy in warehouses and solutions to maximize solar and wind energy use including the optimal solution for the zero energy and near zero climate change impact distribution center network.

The key novelty and contribution presented in this paper was that the study provided a realistic, robust, and systemic approach to improve the environmental sustainability of the distribution centers. The study was based on real distribution center locations and their actual building types and sizes. Energy simulations were based on the warehouse energy consumption survey data. Solar power generation and installation was location-based. Wind turbine installation was based on actual wind speeds, locations, and productivity. Finally, purchased electricity and renewable energy generation and installation costs were based on current state-level prices; thus, providing reliable and current information and solutions for the food distribution industry.

The study linked the whole-building LCA and quantitative analyses including the Monte Carlo uncertainty analysis, Monte Carlo pairwise comparison, and multi-objective optimization. The final selection of better buildings was based on a statistical superiority of the Pareto-optimal solutions over the baseline. The advantage of this approach for a decision-making was that the selected better distribution centers were Pareto-optimal, their environmental performance was statistically better, and they were cost-effective compared to the baseline. The

optimal zero energy distribution centers were the best solutions with regard to current prices, building types, and locations, and had a near zero climate change impact. Thus, the results presented here help understanding the tradeoffs of a potentially feasible zero energy and near zero climate change impact of building-energy systems. While the goal to achieve the zero energy distribution center network remains remote, the proposed better distribution center network could be achievable.

In addition, the results presented in this paper have opened a pathway towards improving the environmental sustainability of food storage in warehouses. Because building and food systems are interconnected in the food-water-energy nexus, the reductions presented in this study should also reduce the environmental impacts of refrigerated and non-refrigerated food storing and handling.

Finally, the study provided new insights into how to interpret and use life cycle assessment results for a decision making and created a paradigm for future research. This research was also in line with several Sustainability Development Goals including climate action and affordable and clean energy goals. The research should be of interest to readers in the areas of building sustainability and complex building-energy system analysis, experts in food distribution sustainability, policy makers, and life cycle assessment experts. Also, the research should be of interest to food supply chain managers for future distribution center planning.

5.1. Future work

The models originating from this research are comprehensive process-based life cycle assessment models, which include accurate and reproducible building energy data. The models can be adapted for any other food supply chain in the world. They allow performing scenario analyses including building performance factors, such as energy efficiency and refrigerator choice and change in building operation technology, energy generation, and supply chain effects. The results can be used to test the environmental and renewable energy policies in place and decision-making.

The methods presented here provide a starting point for further examination of other warehouses. Several conclusions of the study may be valid for similar warehouses in the United States. Solutions for other food distribution centers such as Amazon and Target may be different. Thus, future research should expand to include other businesses. Future research should include analysis what would have to become true to make these solutions feasible. This would enable discussion on what renewable energy policies need to be in place to achieve zero energy distribution center networks in the United States.

The optimization and life cycle impact models presented here can also be adapted to optimize renewable energy in other commercial buildings. The environmental impacts of all supermarkets in the United States were assessed in our previous work. Thus, the future work will extend this research further on finding cost-effective strategies to reduce environmental impacts of supermarkets.

Regional and global consequences of installing new roof solar panels and wind turbines on the energy market were not assessed in this research. The future work should determine the probability of proposed solutions occurring, and consequences of their application using the consequential life cycle assessment. The consequential life cycle assessment, which includes additional economic concepts like marginal production costs, markets, elasticity of supply and demand, and dynamic models, may provide additional insight into what happens with energy markets when the demand for solar energy and wind energy increases.

Practical implementation of solar panels needs to include solar energy storage, which was beyond the scope of this study. Further research is required to evaluate new solar panel, wind turbine, and energy storage technologies. The costs of energy vary; thus, the results presented in the study are true if the prices are not too different. If, for example, wind energy in states for which the current price is lower than purchased grid electricity becomes higher than purchased grid electricity, the Pareto-frontier will change.

Energy efficiency is an important factor in achieving zero energy buildings. The zero energy building will become more feasible only if multiple solutions are offered, which will provide a synergistic effect. Energy efficiency practices in warehousing that could be used in the MOO are: just in time technique (excluding warehouses), skylights, energy storage systems, ground source heat pumps, energy efficient light systems with motion sensors, efficient refrigeration in storage and dock areas and reductions in infiltration rates due to food unloading, sustainable building envelope and insulation material, efficient heating, cooling, and ventilation, as well as other options which may reduce the costs of the proposed zero energy distribution center network.

One potential area of research not discussed in this manuscript is improvements in conveyor efficiency at general merchandise distribution centers. For example, one could use the models to examine the nationwide effect of using more energy-efficient conveyor. However, the biggest challenge is to find life cycle inventories for emerging insulation materials, cold storages, and conveyor.

Other future work may focus on the analysis of different refrigeration systems and refrigerants, which will reduce energy use, climate change impact, and water footprint. However, only the shift to renewable energy can make commercial buildings zero energy and with a minimal GHG impact. In addition to wind and solar energy, we may consider bioenergy produced from food waste, for which knowledge about food waste availability in different regions will be required.

Due to climate change impact the current energy demand of buildings may increase. The models could also be adapted to integrate climate models to assess future distribution centers energy consumption.

One objective that has gained more attention in recent research about buildings and energy is water consumption and water scarcity. Refrigerated buildings use more water, but the challenge is to quantify water losses from different refrigeration system. Rainwater harvesting and an efficient water consumption refrigeration system may be used to reduce purchased water. Adding water consumption and food reductions will contribute in advancing the food-energy-water nexus.

Food refrigeration requirements also affect the refrigeration loads. Refrigerated food may enter a warehouse at a temperature higher than the refrigerated warehouse temperature, which can increase energy consumption. Strategies to reduce energy consumption due to different food temperature requirements and food handling may be another avenue for future research.

In the future, the models and results of this study could be used in a comprehensive decision-making building optimization tool, which will also include renewable energy, other energy efficiency strategies to reduce environmental impact of distribution centers, and indirect effects of food. The hypotheses in the future research will need to be tested through a multi-dimensional optimization model, which will optimize reductions in food, energy, and water nexus to find the better, zero energy and near zero environmental impact distribution centers at a lower cost than proposed in this research. The proposed energy efficiency measures, indirect effects of food, and inclusion of other renewable energy sources could be used to compare different building, food, energy, and water policy regulations.

6. Declarations of interest

None.

This research did not receive any specific grant from funding agencies in the public, commercial, or non-profit sectors.

Appendix A. Supplementary material

Supplementary data to this article can be found online at https://doi.org/10.1016/j.apenergy.2018.11.042.

References

[1] Derrible S, Reeder M. The cost of over-cooling commercial buildings in the United States. Energy Build 2015;108:304–6. https://doi.org/10.1016/j.enbuild.2015.09.022.

[2] Ibn-Mohammed T, Greenough R, Taylor S, Ozawa-Meida L, Acquaye A. Operational vs. embodied emissions in buildings – a review of current trends. Energy Build 2013;66:232–45. https://doi.org/10.1016/j.enbuild.2013.07.026.

[3] Wang B, Xia X, Zhang J. A multi-objective optimization model for the life-cycle cost analysis and retrofitting planning of buildings. Energy Build 2014;77:227–35. https://doi.org/10.1016/j.enbuild.2014.03.025.

[4] Zhu K, Li X, Campana PE, Li H, Yan J. Techno-economic feasibility of integrating energy storage systems in refrigerated warehouses. Appl Energy 2018. https://doi.org/10.1016/j.apenergy.2018.01.079.

[5] Reindl D, Claas M, Denison J. Prospects of powering a refrigerated warehouse with renewable energy. ASHRAE J 2018.

[6] Fikiin K, Stankov B, Evans J, Maidment G, Foster A, Brown T, et al. Refrigerated warehouses as intelligent hubs to integrate renewable energy in industrial food refrigeration and to enhance power grid sustainability. Trends Food Sci Technol 2017;60:96–103. https://doi.org/10.1016/j.tifs.2016.11.011.

[7] Meneghetti A, Dal Magro F, Simeoni P. Fostering renewables into the cold chain: how photovoltaics affect design and performance of refrigerated automated warehouses. Energies 2018. https://doi.org/10.3390/en11051029.

[8] Fan Y, Xia X. A multi-objective optimization model for energy-efficiency building envelope retrofitting plan with rooftop PV system installation and maintenance. Appl Energy 2017. https://doi.org/10.1016/j.apenergy.2016.12.077.

[9] Safaei A, Freire F, Henggeler Antunes C. A life cycle multi-objective economic and environmental assessment of distributed generation in buildings. Energy Convers Manag 2015;97:420–7. https://doi.org/10.1016/j.enconman.2015.03.048.

[10] Jing R, Wang M, Wang W, Brandon N, Li N, Chen J, et al. Economic and environmental multi-optimal design and dispatch of solid oxide fuel cell based CCHP system. Energy Convers Manag 2017;154:365–79. https://doi.org/10.1016/j.enconman.2017.11.035.

[11] U.S. Green Building Council. Leadership in energy and environmental design (LEED) v4. 2013. http://www.usgbc.org/leed (accessed June 5, 2017).

[12] Carreras J, Pozo C, Boer D, Guillen-Gosalbez G, Caballero JA, Ruiz-Femenia R, et al. Systematic approach for the life cycle multi-objective optimization of buildings combining objective reduction and surrogate modeling. Energy Build 2016;130:506–18. https://doi.org/10.1016/j.enbuild.2016.07.062.

[13] NREL. Cost Control Strategies for Zero Energy Buildings; 2015.

[14] Miller TR, Gregory J, Kirchain R. Critical Issues When Comparing Whole Building & Building Product Environmental Performance; 2016.

[15] Ostermeyer Y, Wallbaum H, Reuter F. Multidimensional Pareto optimization as an approach for site-specific building refurbishment solutions applicable for life cycle sustainability assessment. Int J Life Cycle Assess 2013;18:1762–79. https://doi.org/10.1007/s11367-013-0548-6.

[16] Antipova E, Boer D, Guillén-Gosálbez G, Cabeza LF, Jiménez L. Multi-objective optimization coupled with life cycle assessment for retrofitting buildings. Energy Build 2014;82:92–9. https://doi.org/10.1016/j.enbuild.2014.07.001.

[17] Mariaud A, Acha S, Ekins-Daukes N, Shah N, Markides CN. Integrated optimisation of photovoltaic and battery storage systems for UK commercial buildings. Appl Energy 2017. https://doi.org/10.1016/j.apenergy.2017.04.067.

[18] Wang JJ, Yang K, Xu ZL, Fu C, Li L, Zhou ZK. Combined methodology of optimization and life cycle inventory for a biomass gasification based BCHP system. Biomass Bioenergy 2014;67:32–45. https://doi.org/10.1016/j.biombioe.2014.03.026.

[19] Negendahl K, Nielsen TR. Building energy optimization in the early design stages: a simplified method. Energy Build 2015;105:88–99. https://doi.org/10.1016/j.enbuild.2015.06.087.

[20] Charitopoulos VM, Dua V. A unified framework for model-based multi-objective linear process and energy optimisation under uncertainty. Appl Energy 2017. https://doi.org/10.1016/j.apenergy.2016.05.082.

[21] Wang J, Yang Y, Mao T, Sui J, Jin H. Life cycle assessment (LCA) optimization of solar-assisted hybrid CCHP system. Appl Energy 2015. https://doi.org/10.1016/j.apenergy.2015.02.056.

[22] Karan E, Mohammadpour A, Asadi S. Integrating building and transportation energy use to design a comprehensive greenhouse gas mitigation strategy. Appl Energy 2016;165:234–43. https://doi.org/10.1016/j.apenergy.2015.11.035.

[23] Validi S, Bhattacharya A, Byrne PJ. A case analysis of a sustainable food supply chain distribution system – a multi-objective approach. Int J Prod Econ 2014;152:71–87. https://doi.org/10.1016/j.ijpe.2014.02.003.

[24] Burek J, Nutter D. Environmental Performance of Chilled and Frozen Food Storing and Retailing (Manuscript submitted for publication); 2018.

[25] Chau CK, Leung TM, Ng WY. A review on life cycle assessment, life cycle energy assessment and life cycle carbon emissions assessment on buildings. Appl Energy 2015;143:395–413. https://doi.org/10.1016/j.apenergy.2015.01.023.

[26] Abd Rashid AF, Yusoff S. A review of life cycle assessment method for building industry. Renew Sustain Energy Rev 2015;45:244–8. https://doi.org/10.1016/j.rser.2015.01.043.

[27] Cabeza LF, Rincón L, Vilariño V, Pérez G, Castell A. Life cycle assessment (LCA) and life cycle energy analysis (LCEA) of buildings and the building sector: a review. Renew Sustain Energy Rev 2014;29:394–416. https://doi.org/10.1016/j.rser.2013.08.037.

[28] Richman R, Pasqualini P, Kirsh A. Life-cycle analysis of roofing insulation levels for cold storage buildings. J Archit Eng 2009;15:55–61. https://doi.org/10.1061/(ASCE)1076-0431(2009) 15:2(55).

[29] DOE. Zero Energy Buildings; 2018. https://www.energy.gov/eere/buildings/zero-energy-buildings (accessed October 2, 2018).

[30] Cao S, Alanne K. The techno-economic analysis of a hybrid zero-emission building system integrated with a commercial-scale zero-emission hydrogen vehicle. Appl Energy 2018. https://doi.org/10.1016/j.apenergy.2017.11.079.

[31] Weißenberger M, Jensch W, Lang W. The convergence of life cycle assessment and nearly zero-energy buildings: the case of Germany. Energy Build 2014;76:551–7. https://doi.org/10.1016/j.enbuild.2014.03.028.

[32] Hernandez P, Kenny P. From net energy to zero energy buildings: defining life cycle zero energy buildings (LC-ZEB). Energy Build 2010;42:815–21. https://doi.org/10.1016/j.enbuild.2009.12.001.

[33] Brinks P, Kornadt O, Oly R. Development of concepts for cost-optimal nearly zero-energy buildings for the industrial steel building sector. Appl Energy 2016. https://doi.org/10.1016/j.apenergy.2016.04.007.

[34] Burek J, Nutter D. Life cycle assessment of grocery, perishable, and general merchandise multi-facility distribution center networks. Energy Build 2018. https://doi.org/10.1016/j.enbuild.2018.06.021.

[35] Alegria A. Reconstruction era : Recovery makes its way as vacancy rates fall and corporate profit returns Commercial Building Construction in the US About this Industry; 2012. p. 1–35.

[36] US EIA. 2012 Commercial Buildings Energy Consumption Survey: Energy Usage Summary; 2016.

[37] MWPVL International. The gorcery distribution network in North America 2010. http://www.mwpvl.com/html/grocery_distribution_network.html (accessed November 2, 2015).

[38] US EIA. Use of Electricity 2017. https://www.eia.gov/energyexplained/print.php?page=electricity_use (accessed September 5, 2018).

[39] Chan FTS, Chan HK. The future trend on system-wide modelling in supply chain studies. Int J Adv Manuf Technol 2005;25:820–32. https://doi.org/10.1007/s00170-003-1851-3.

[40] MWPVL International. The Walmart Distribution Center Network in the United States. MWPVL Int 2013:1–34. http://www.mwpvl.com/html/walmart.html (accessed August 10, 2016).

[41] USDA NASS. Cold Storage 2017 Summary; 2018.

[42] US-DOE. EnergyPlus Energy Simulation Software; 2015.

[43] ISO. ISO 14040:2006 – Environmental management – Life cycle assessment – Principles and framework 2006. http://www.iso.org/iso/catalogue_detail?csnumber=37456 (accessed February 22, 2017).

[44] ISO. ISO 14044:2006 – Environmental management – Life cycle assessment – Requirements and guidelines 2006. http://www.iso.org/iso/home/store/catalogue_tc/catalogue_detail.htm?csnumber=38498 (accessed February 22, 2017).

[45] ISO. ISO 14046:2014 – Environmental management – Water footprint – Principles, requirements and guidelines 2014. http://www.iso.org/iso/home/store/catalogue_tc/catalogue_detail.htm?csnumber=43263 (accessed February 22, 2017).

[46] PRé Consultants. SimaPro 8.4. software; 2015.

[47] Hu M, Cho H. A probability constrained multi-objective optimization model for CCHP system operation decision support. Appl Energy 2014. https://doi.org/10.1016/j.apenergy.2013.11.065.

[48] Wang H, Zhai (John) Z. Advances in building simulation and computational techniques: a review between 1987 and 2014. Energy Build 2016(128):319–35. https://doi.org/10.1016/j.enbuild.2016.06.080.

[49] MathWorks. Matlab documentation: multi-objective goal attainment optimization; 2015.

[50] U.S. Energy Infromation Administration. State electricity profiles. Data for 2016; 2016; 0348: 1–314. http://www.eia.gov/electricity/state/pdf/sep2010.pdf.

[51] Lazard. Levelised cost of energy analysis; 2017.

[52] EnergySage. What will a 10,000 Watt (10 kW) solar system cost in your state in 2018 ? 2018: 1–5.

[53] Solar Power Rocks. How many solar panels do you need? 2018:1–15. https://solarpowerrocks.com/square-feet-solar-roof/.

[54] Solar Power Rocks. How many solar panels do you need? 2018: 1–15.

[55] Interstate Renewable Energy Council. Solar photovoltaic installation guideline; 2008.

[56] Google Ink. Project Sunroof data explorer: a description of methodology and inputs; 2017: 1–6.

[57] Mission O, Policy S, Solar O, Leases S. How to calculate the amount of kilowatt hours (kWh) your solar panel system will produce; 2018: 1–12.

[58] Huijbregts MaJ, Rombouts LJa, Hellweg S, Frischknecht R, Hendriks aJ, Van de Meent D, et al. Is cumulative fossil energy demand a useful indicator for the environmental performance of products? Environ Sci Technol 2006;40:641–8.

[59] Hischier R, Weidema B, Althaus H-J, Bauer C, Doka G, Dones R, et al. Implementation of life cycle impact assessment methods. Data v2.2 (2010). Dubendorf, Switzerland: Swiss Centre for Life Cycle Inventories; 2010.

[60] Hodnebrog Etminan M, Fuglestvedt JS, Marston G, Myhre G, Nielsen CJ, Shine KP, et al. Global warming potentials and radiative efficiencies of halocarbons and related compounds: a comprehensive review. Rev Geophys 2013. https://doi.org/10.1002/rog.20013.

[61] LTS. DATASMART LCI Package (US-EI SimaPro® Library); 2016. https://

earthshiftsustainability.com/services/software/datasmart-life-cycle-inventory/.
[62] Eisenhower B, Neill ZO, Fonoberov VA, Mezi I. Uncertainty and sensitivity decomposition of building energy models. J Build Perform Simul 2011;00:1–18. https://doi.org/10.1080/1940149YYxxxxxxxx.
[63] Greenhouse Gas Protocol. Quantitative inventory uncertainty. vol. 2; 2007.
[64] Frischknecht R, Jungbluth N, Althaus H, Bauer C, Doka G, Dones R, et al. Ecoinvent 2.2: Code of practice - data v2.0 (2007). Dubendorf, Switzerland: Swiss Centre for Life Cycle Inventories; 2007.
[65] Weidema BP. Guidelines for critical review of product LCA. SPOLD, Brussels; 1997: 14.
[66] Peterson K, Taylor C, Grant R. Establishing a common definition for zero energy buildings: time to move the market; 2016.
[67] NREL. New national wind potential estimates for modern and near-future turbine technologies; 2014.
[68] Lippiatt BC, Kneifel JD, Lavappa PD, Suh S, Greig AL. Building Industry Reporting and Design for Sustainability (BIRDS). Technical Manual and User Guide. 2013. doi: 914484.